(Supplementary Material) Computational modelling of attentional selectivity in depression reveals perceptual deficits

James A. Grange
School of Psychology, Keele University, UK

Michelle Rydon-Grange
Midlands Partnership Foundation NHS Trust, UK

Appendix A
Model Details

This section provides a more comprehensive account of the dual-stage two phase (DSTP) model (Hübner, Steinhauser, & Lehle, 2010) and the shrinking spotlight (SSP) model (White, Ratcliff, & Starns, 2011). We describe how each model accounts for the improvement of attentional selectivity with time, as well as a more detailed overview of the latent parameters estimated by the model fitting routine.

DSTP Model

The model assumes that response selection proceeds according to a drift diffusion process, which is shown schematically in Figure A1. After perceptual encoding of the stimulus, noisy evidence is accumulated towards one of two response boundaries, one of which represents the correct response and the other represents the incorrect response (see upper panel of Figure A1). The height of the correct response boundary is determined by the model parameter A, and the height of the incorrect response boundary is set by the model parameter $B = -A$.

At early stages of processing, response selection is poor because it is influenced by both the central target and the flanker stimuli. Specifically, the drift rate—that is, the rate at which the diffusion process rises to one of the two response boundaries—is determined by the additive combination of model parameters μ_{TA} and mu_{FL} representing the contributions of both the target and the flanker stimuli to response selection. On congruent trials, this contribution from the flanker stimuli to the drift rate facilitates response speed and accuracy because the information is congruent with the desired response. However, on incongruent trials, the contribution of mu_{Fl} to the drift rate is detrimental. Specifically, on incongruent trials mu_{Fl} takes on a negative value, and is positive on congruent trials.

In parallel to the response selection process, late attentional processes work to select a single item from the stimulus display for more detailed processing. This stimulus selection phase is also modelled by a diffusion process (see the bottom panel of Figure A1), and thus the time it takes the cognitive system to select a stimulus for further processing is explicitly modelled. Evidence is accumulated in a noisy fashion towards one of two absorbing boundaries, the drift rate of which is determined by the model parameter μ_{SS}. If the upper boundary is reached by the diffusion process, it is assumed that the model has selected the central target for further processing; if the diffusion process reaches the lower panel it is assumed the model has erroneously selected one of the flankers for further processing. The height of the stimulus selection boundary representing a target selection is set to C; the height of the boundary representing selection of a flanker is set to $D = -C$.

If the stimulus selection process finishes before the response selection process, response selection enters its second stage, which is highly selective. Specifically, the drift rate for response selection in Stage 2 is determined solely by which stimulus was selected by the stimulus selection process. If the model selected the central target for processing, the drift rate for Stage 2 of the response selection process increases leading to a sharper rise of the diffusion process towards the correct response boundary (see the example in Stage 2 of the upper panel in Figure A1). If, however, the stimulus selection process erroneously selects one of the flankers for further processing, the drift rate for Stage 2 of the response selection process becomes negative, meaning the diffusion process will march rapidly towards the

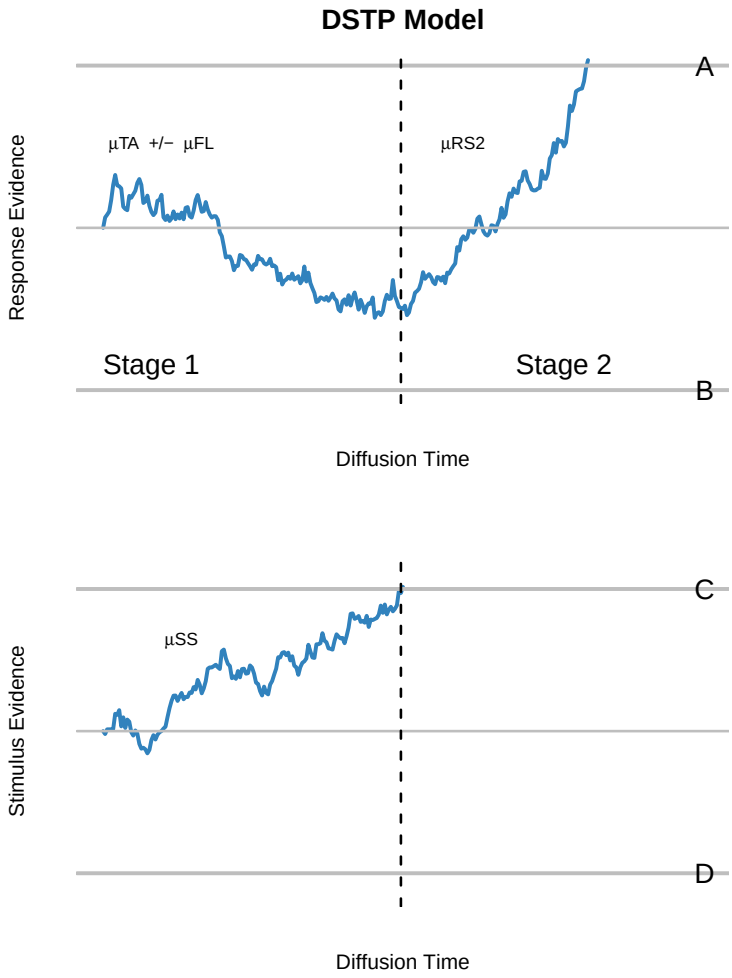

Figure A1. Schematic overview of the parallel drift diffusion processes in the Dual Stage Two Phase (DSTP) model for one trial. The upper panel depicts the diffusion process for response selection, and the lower panel depicts the diffusion process for stimulus selection. The point in time that a stimulus is selected for further processing is depicted by the dashed vertical line. The diffusion process before this point represents the first stage of response selection, and after this point represents the second—more selective—stage of response selection. See text for details.

incorrect response boundary. The drift rate for this second stage of response selection is determined by the model parameter μ_{RS2}, which is set to positive if the target is selected, and negative if a flanker is selected.

The final parameter in the DSTP model is *ter*, which captures all non-decisional components of response time, such as the time taken for motoric responding.

SSP Model

The shrinking spotlight model also assumes that response selection proceeds according to a drift diffusion process (see upper panel of Figure A2), with the same absorbing response boundaries as the DSTP model. The height of the response boundary for the correct response is represented by the model parameter A, and the height of the incorrect response boundary is set to $B = -A$.

Attentional selectivity increases with time, and this increased selectivity leads to an increase in the drift rate of the diffusion process across time—$v(t)$—as seen in Figure A2. The drift rate is determined by the strength of the perceptual input of each stimulus item in the display (i.e., target and flankers) multiplied by the proportion of attention currently being paid to each element in the display. As time progresses, more attention is paid to the central target stimulus, which means that as time progresses the drift rate is determined more by the target and less by the flanker stimuli; the net effect is an increase in attentional selectivity with time.

This change in attentional selectivity is shown schematically in the lower panel of Figure A2. The left plot in the lower panel of Figure A2 shows the distribution of attention across the stimulus display at early stages of processing. The distribution of attentional focus (i.e., the attentional spotlight) is modelled by a normal distribution centered on the target stimulus. The height of the distribution models how much attention is paid to each element in the display. At early stages of processing, a non-trivial amount of attention is paid to the flankers. As time progresses (from left to right in the Figure), the width of this attentional distribution narrows, meaning more attention is paid to the central target.

Formally, this reduction of the width of the attentional distribution is modelled by a reduction of the standard deviation of the normal distribution across time; the standard deviation of the attentional distribution at time t, $sd_a(t)$ is given by

$$sd_a(t) = sd_a - r_d t, \tag{1}$$

where the model parameter r_d captures the rate of the reduction at time t; larger values of r_d thus reflect faster focusing on the central target.

Given the above assumptions, and assuming each stimulus in the display is one unit wide, the total attention being paid to the outer flankers (a_{outer}), the inner flankers (a_{inner}), and the central target (a_{target}) at time t is given by

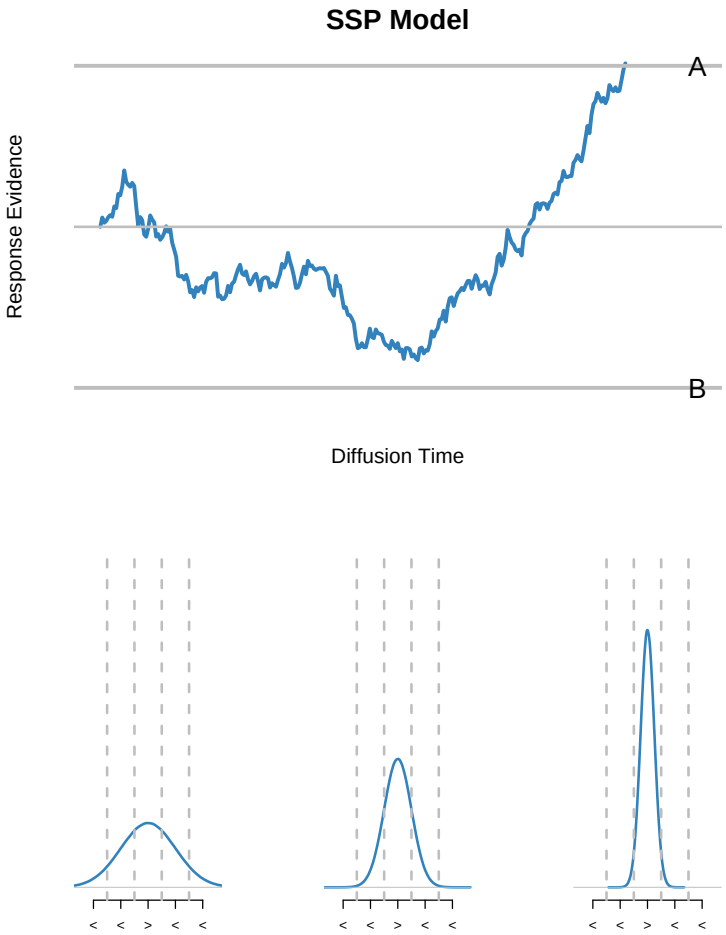

Figure A2. Schematic overview of the diffusion process for response selection in the shrinking spotlight (SSP) model. The upper panel depicts the diffusion process for response selection, the drift rate of which is determined by the perceptual input of stimuli that fill within the area of the attentional spotlight, depicted in the lower panel. As time progresses, the attentional spotlight becomes more focussed around the central target, meaning perceptual information from the flankers contribute less to the drift rate of response selection as time increases.

$$
\begin{aligned}
a_{outer}(t) &= \int_{1.5}^{\infty} \phi[0, sd_a(t)]; \\
a_{inner}(t) &= \int_{0.5}^{1.5} \phi[0, sd_a(t)]; \\
a_{target}(t) &= \int_{-0.5}^{0.5} \phi[0, sd_a(t)].
\end{aligned} \tag{2}
$$

Here, ϕ is the density function for the normal distribution with mean 0 and standard deviation of $sd_a(t)$ (see Equation 1). As mentioned earlier, the drift rate for response selection is a multiplicative combination of the perceptual strength, p, of each element in the stimulus display and the amount of attention, a_x, currently being paid to each element. The perceptual strength parameter p for all items in a congruent stimulus is set to positive; for incongruent stimuli, only the central item takes a positive value for p and the flankers take on a value of $-p$.

The drift rate at time t, $v(t)$, is given by

$$
v(t) = 2p_{outer}a_{outer}(t) + 2p_{inner}a_{inner}(t) + p_{target}a_{target}(t). \tag{3}
$$

Gaussian noise is then added to this drift rate. The SSP model also has a non-decisional parameter *ter* which is interpreted identically to the DSTP model.

Appendix B
Questionnaire Analysis

This section presents the plots of the Bayesian regressions examining the relationship between QIDS and SHPS scores across all three experiments. As can be seen in Figures B1–B3 there was good variability and ranges of scores across all three experiments for both the QIDS and the SHPS scores. Bayesian regressions showed that QIDS scores were positively predicted by SHPS scores across all three experiments, indicating good convergence (see main text for more details).

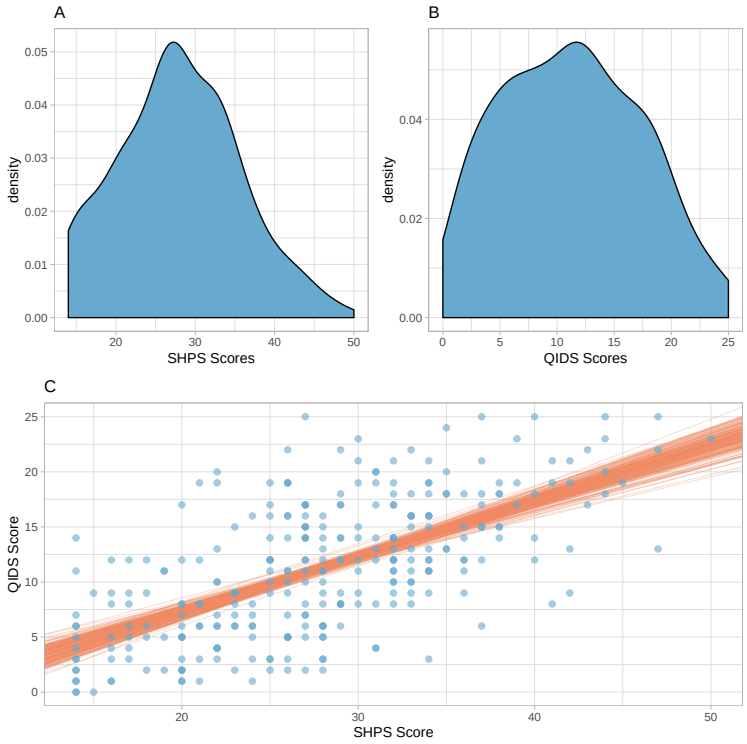

Figure B1. Experiment 1 data. A. Density distribution of scores on the SHPS questionnaire. B. Density distribution of scores on the QIDS questionnaire. C. Points show individual participants' QIDS score plotted against their SHPS score. The lines represent 200 draws from the posterior distribution of a Bayesian linear regression predicting QIDS scores from SHPS scores.

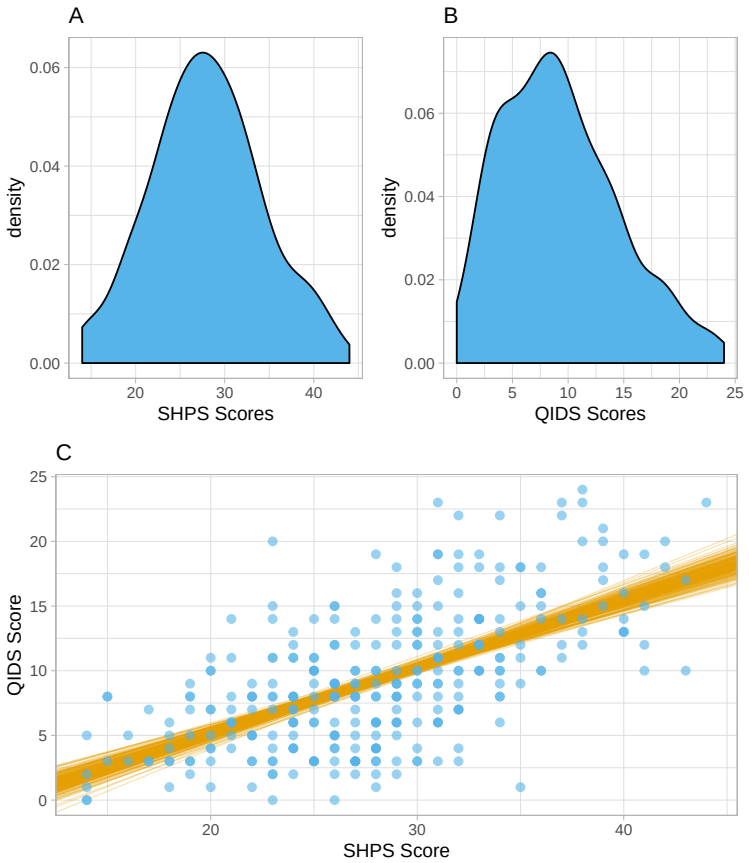

Figure B2. Experiment 2 data. A. Density distribution of scores on the SHPS questionnaire. B. Density distribution of scores on the QIDS questionnaire. C. Points show individual participants' QIDS score plotted against their SHPS score. The lines represent 200 draws from the posterior distribution of a Bayesian linear regression predicting QIDS scores from SHPS scores.

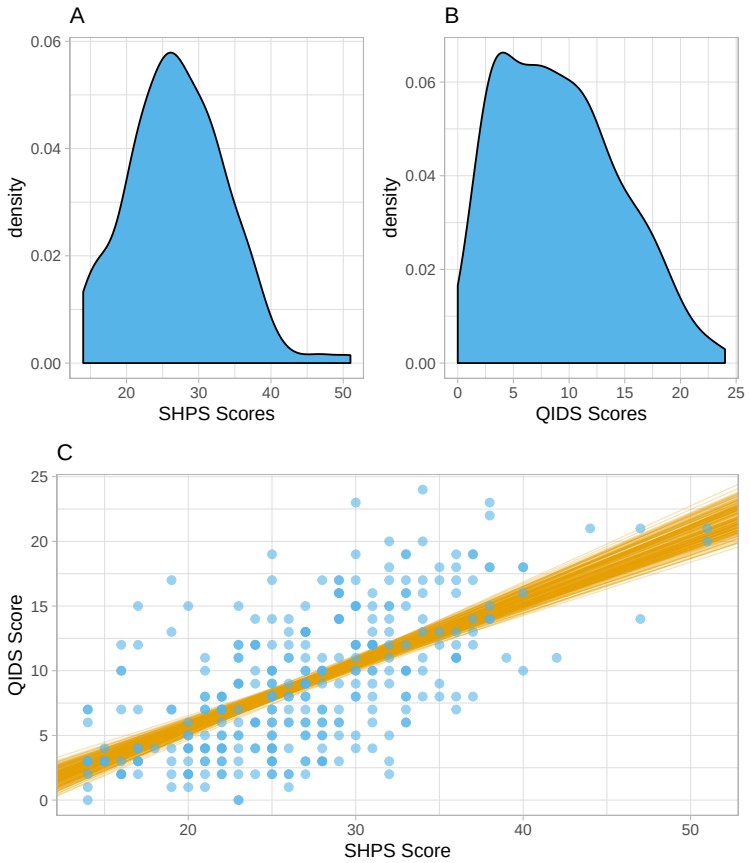

Figure B3. Experiment 3 data. A. Density distribution of scores on the SHPS questionnaire. B. Density distribution of scores on the QIDS questionnaire. C. Points show individual participants' QIDS score plotted against their SHPS score. The lines represent 200 draws from the posterior distribution of a Bayesian linear regression predicting QIDS scores from SHPS scores.

Appendix C
Expanded Detail of Behavioural Data Analysis

In this section we provide additional details of the analyses of the behavioural data, together with the regressions with questionnaire scores. Figures C1–C3 show density distributions of the behavioural data in Experiments 1–3 respectively for both response time and accuracy data. These plots demonstrate good data quality in that there is low variance in the RTs, and excellent accuracy performance.

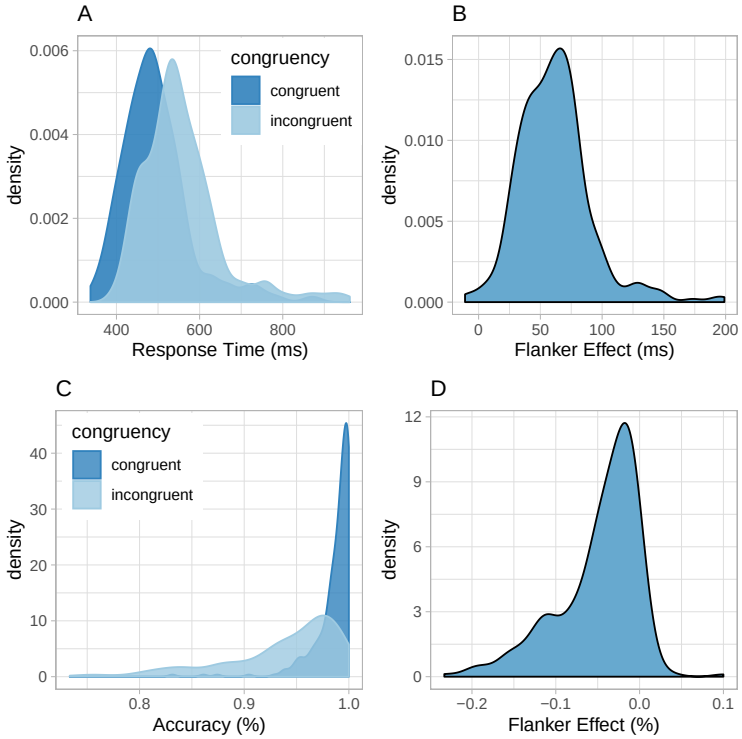

Figure C1. Density distributions of the behavioural data in Experiment 1. Panel A: Density distributions of congruent and incongruent response time (in milliseconds, ms). Panel B: Density distributions of the flanker effect for response time data (RT incongruent – RT congruent). Panel C: Density distribution of the congruent and incongruent accuracy. Panel D: Density distribution of the flanker effect in accuracy.

Table C1 shows all model parameters for the Bayesian regressions conducted predicting behavioural data from questionnaire scores. Note that in this table we also present regressions predicting mean RT and mean accuracy from the questionnaire scores, which is not reported in the main paper. Figures C4–C6 plot the relationship between flanker effects in RT and accuracy and scores on the QIDS and SHPS, together with draws from the posterior distribution of the Bayesian regression model fits.

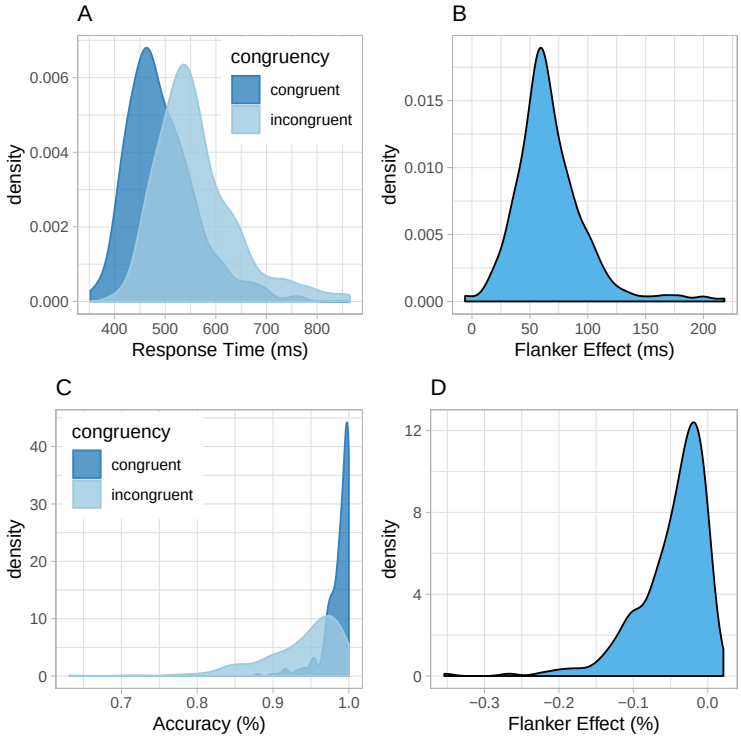

Figure C2. Density distributions of the behavioural data in Experiment 2. Panel A: Density distributions of congruent and incongruent response time (in milliseconds, ms). Panel B: Density distributions of the flanker effect for response time data (RT incongruent – RT congruent). Panel C: Density distribution of the congruent and incongruent accuracy. Panel D: Density distribution of the flanker effect in accuracy.

Table C1

Regression coefficients for the series of Bayesian regressions predicting behavioural dependent variables (DV) from QIDS and SHPS questionnaire scores across all Experiments. The values represent the mean estimate of the posterior distribution for each coefficient, together with their 95% credible interval in square parentheses.

		QIDS		SHPS	
Experiment	DV	$\beta_{Intercept}$	β_{QIDS}	$\beta_{Intercept}$	β_{SHPS}
E1	Mean RT	524.27 [506.95, 541.97]	-0.11 [-1.40, 1.20]	552.71 [523.62, 580.63]	-1.07 [-2.04, -0.09]
	Flanker RT	61.13 [53.77, 68.36]	0.02 [-0.53, 0.58]	63.44 [58.70, 68.17]	-0.65 [-1.67, 0.40]
	Mean Acc.	0.962 [0.957, 0.966]	-0.0002 [-0.0005, 0.0000]	0.959 [0.951, 0.968]	0.0000 [-0.0003, 0.0003]
	Flanker Acc.	-0.047 [-0.057, -0.037]	-0.0003 [-0.0010, 0.0005]	-0.049 [-0.056, -0.043]	-0.0003 [-0.0015, 0.0009]
E2	Mean RT	533.43 [519.16, 548.11]	-0.91 [-2.20, 0.36]	531.29 [501.78, 562.19]	-0.23 [-1.30, 0.80]
	Flanker RT	65.34 [58.31, 72.25]	0.23 [-0.41, 0.89]	72.23 [56.62, 87.76]	-0.17 [-0.71, 0.38]
	Mean Acc.	0.960 [0.956, 0.964]	-0.0001 [-0.0005, 0.0002]	0.960 [0.956, 0.968]	0.0000, [-0.0003, 0.0002]
	Flanker Acc.	-0.048 [-0.055, -0.041]	-0.0003 [-0.0009, 0.0003]	-0.051 [-0.065, -0.037]	0.0000 [-0.0005, 0.0004]
E3	Mean RT	512.69 [499.07, 526.09]	0.20 [-1.05, 1.44]	509.69[480.57, 538.19]	0.18 [-0.84, 1.22]
	Flanker RT	34.41 [30.79, 37.84]	0.11 [-0.22, 0.44]	36.51 [29.58, 43.52]	-0.04 [-0.29, 0.21]
	Mean Acc.	0.961 [0.957, 0.965]	-0.0002 [-0.0006, 0.0001]	0.962 [0.955, 0.969]	-0.0001, [-0.0003, 0.0001]
	Flanker Acc.	-0.042 [-0.048, -0.037]	0.0001 [-0.0004, 0.0007]	-0.048[-0.058, -0.037]	0.0002 [-0.0001, 0.0006]

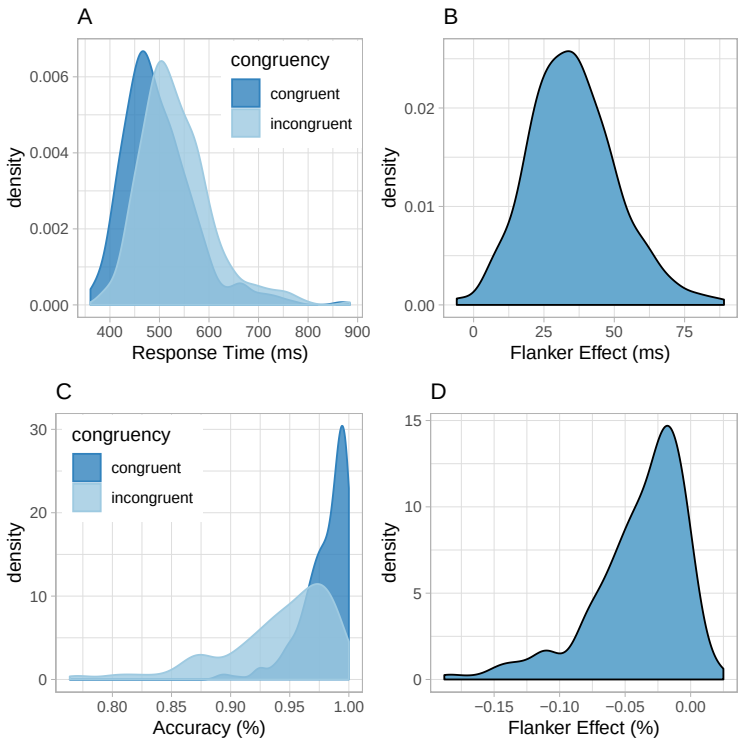

Figure C3. Density distributions of the behavioural data in Experiment 3. Panel A: Density distributions of congruent and incongruent response time (in milliseconds, ms). Panel B: Density distributions of the flanker effect for response time data (RT incongruent – RT congruent). Panel C: Density distribution of the congruent and incongruent accuracy. Panel D: Density distribution of the flanker effect in accuracy.

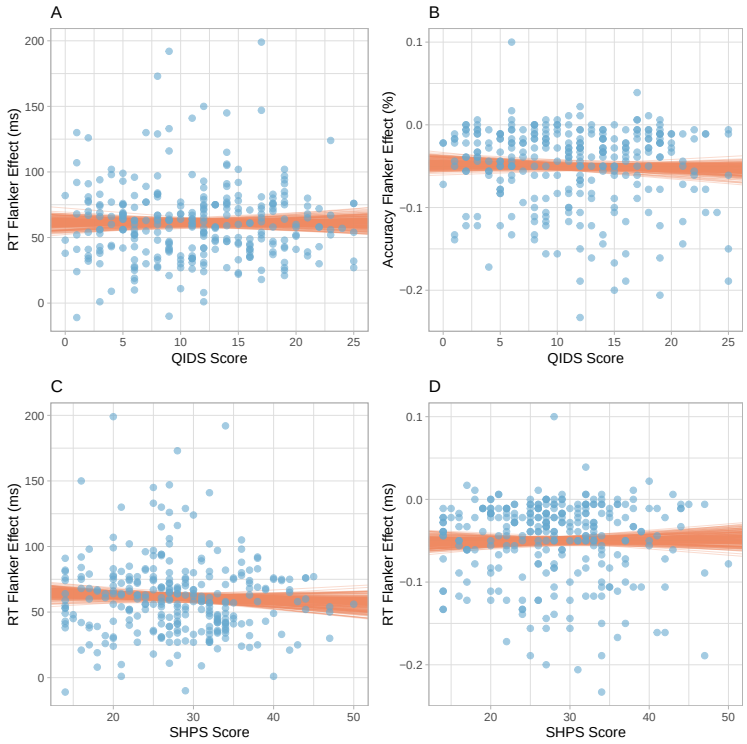

Figure C4. Behavioural flanker effects predicted from questionnaire scores in Experiment 1. Points represent individual participant data; lines represent 200 draws from the posterior distribution of the Bayesian regression model, showing credible estimates of the linear relationship. Panel A: Flanker effect in response time predicted from the QIDS questionnaire. Panel B: Flanker effect in accuracy predicted from the QIDS questionnaire. Panel C: Flanker effect in response time predicted from the SHPS questionnaire. Panel D: Flanker effect in accuracy predicted from the SHPS questionnaire.

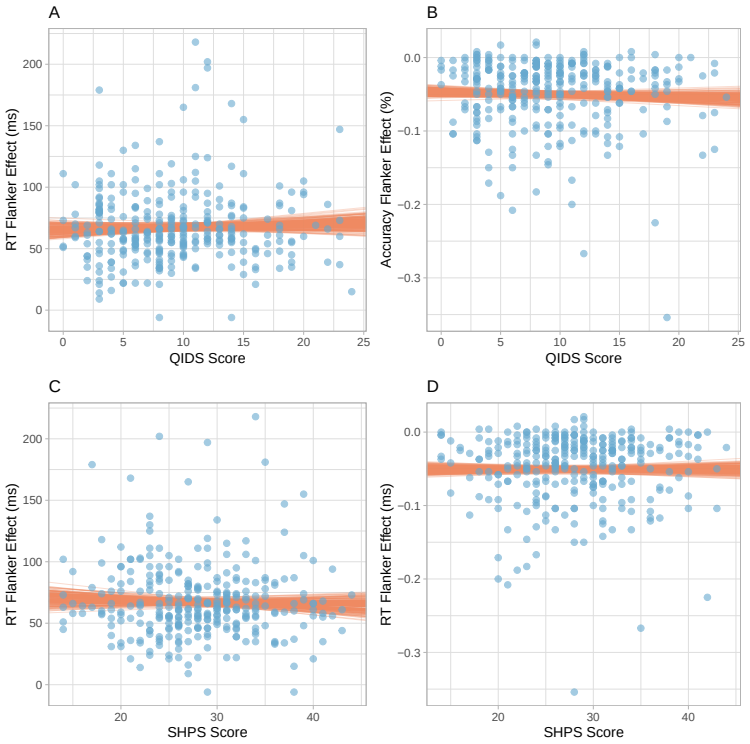

Figure C5. Behavioural flanker effects predicted from questionnaire scores in Experiment 2. Points represent individual participant data; lines represent 200 draws from the posterior distribution of the Bayesian regression model, showing credible estimates of the linear relationship. Panel A: Flanker effect in response time predicted from the QIDS questionnaire. Panel B: Flanker effect in accuracy predicted from the QIDS questionnaire. Panel C: Flanker effect in response time predicted from the SHPS questionnaire. Panel D: Flanker effect in accuracy predicted from the SHPS questionnaire.

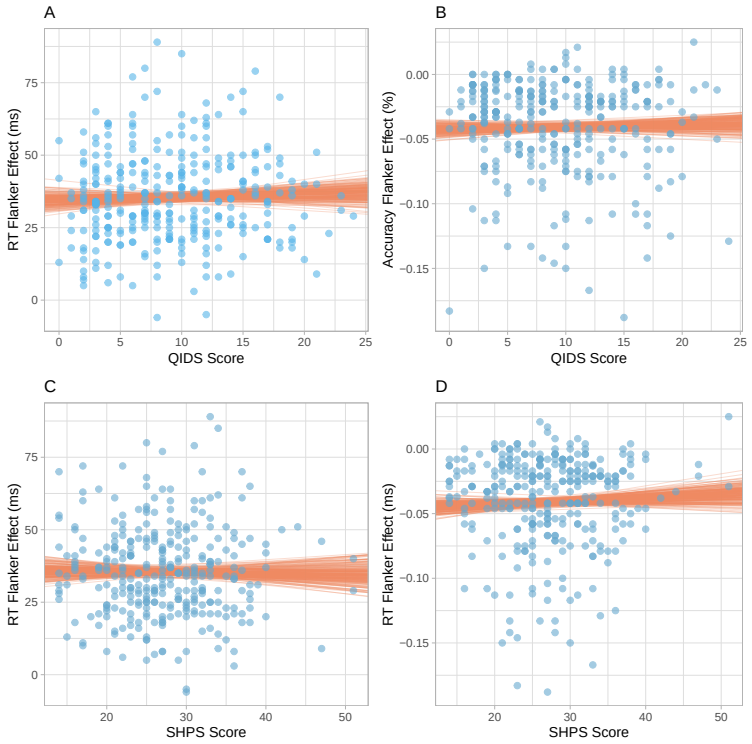

Figure C6. Behavioural flanker effects predicted from questionnaire scores in Experiment 3. Points represent individual participant data; lines represent 200 draws from the posterior distribution of the Bayesian regression model, showing credible estimates of the linear relationship. Panel A: Flanker effect in response time predicted from the QIDS questionnaire. Panel B: Flanker effect in accuracy predicted from the QIDS questionnaire. Panel C: Flanker effect in response time predicted from the SHPS questionnaire. Panel D: Flanker effect in accuracy predicted from the SHPS questionnaire.

Appendix D
Model Fitting and Goodness of Fit Assessment

This section provides more detail on how the computational models were fit to the participant data together with assessment of the goodness of fit to the behavioural data.

Description of Model Fit Routine

As described in Grange (2016), the models are fitted to response time and accuracy distributions: specifically, the model is fitted to cumulative distribution functions (CDFs) of correct response time, and conditional accuracy functions (CAFs), which combine accuracy and response time information. CDFs and CAFs are created for each condition of congruency separately, for each participant. CDFs are constructed by finding the response time cut-off points for the 0.1, 0.3, 0.5, 0.7, and 0.9 quantiles of the correct response time distribution. Conditional accuracy functions are generated by ordering the complete data (i.e., error and correct trials) according to the response time (from fastest to slowest). This data is then partitioned into four bins, each containing 25% of data. For each bin, mean response time and percent accuracy is calculated. CAFs thus assess how accuracy changes with response time.

The fit routine in `flankr` finds the set of parameters that generates simulated CDFs and CAFs that match the participant data. The fit routine aims to minimsie the discrepancy between the simulated and observed CDFs and CAFs, by aiming to minimise the likelihood ratio chi-square statistic, G^2:

$$G^2 = 2\sum_{i}^{J} N p_i ln\left(\frac{p_i}{\pi_i}\right). \tag{4}$$

In Equation 4, p_i is the proportion of observations in the ith bin (i.e., across CDFs and CAFs) for participants, π_i is the proportion in this bin in the simulated model data, N is the average number of trials (which is set to 250 in `flankr`, J is the total number of bins, and ln is the natural logarithm.

The fit routine aims to find the best set of parameters that minimises the G^2 statistic. Recall that the models were fit to each participant's data individually. In order to avoid local minima, the fit routine occurred in two stages. In the first stage, we conducted a broad search of the parameter space by starting the fit routine from 50 random starting points. During this initial exploration, we simulated 1,000 data points from the model on each iteration of the fit routine. The best-fitting parameters from this first stage were then entered as the starting parameters in the final fitting stage, which simulated 50,000 data points per iteration of the fit routine. The best-fitting parameters from this final stage were stored as the best parameters for that particular participant. This procedure was used for each participant individually for both models.

Goodness of Fit Assessment

The goodness of fit of the model to participant data was assessed visually using QQ-plots of model predictions against participant data. Specifically, for each participant, for each condition of congruency, and for each model, we simulated data using that participant's best-fitting model parameters (simulating 50,000 trials); for both the model's simulated data

and the participant's data, we calculated total proportion accuracy, and the 25th, 50th, and 75th quantile of the correct response time distribution. These values were plotted against each other (on four separate plots). This process was then repeated for all participants.

The results of this procedure can be seen in Figures D1–D3 for Experiments 1–3 respectively. In these plots, each point shows the model's prediction plotted against the participant's data; if model predictions are perfect, all data points should lie across the dashed diagonal line. As can be seen, the model predictions (for both the DSTP and SSP) fit the participant data well across all 3 Experiments.

Comparing Model Fit

As both models were fit to individual participant data, we wanted to explore whether one particular model proved superior fits over the other. We therefore wanted to compare the fit statistic G^2 for the DSTP and SSP models across all participants. Recall that lower G^2 values indicate better fit, which can be useful for comparing the fit of two (or more) models; however, the DSTP has more parameters (7) than the SSP model (5), and—all else being equal—models with more parameters fit data better than models with fewer parameters.

We therefore used the Bayesian Information Criterion for binned data—bBIC—which includes a penalty term for the number of parameters in each model; this statistic provides a measure of the goodness of fit whilst controlling for the number of parameters in the model. Lower values of bBIC indicate superior fit; therefore, we wished to compare bBIC scores for the DSTP model and the SSP model across participants.

bBIC is given by

$$\text{bBIC} = -2\left(\sum_{i}^{J} Np_i ln(\pi_i)\right) + Mln(N), \tag{5}$$

where M is the number of parameters in the model; all other terms are equivalent to those in Equation 4.

We calculated bBIC for each participant for each model, and plotted them against each other (see the upper panel of Figures D4–D6). Those data points that are plotted above the diagonal represent participants whose data were better explained by the DSTP model, and those below the diagonal represent participants whose data were better explained by the SSP model. The lower panel of Figures D4–D6 is a different representation of the same data; it plots the difference in bBIC scores—delta bBIC—calculated by bBIC(DSTP) - bBIC(SSP). Postive values of delta bBIC represent superior fit of the SSP model, and negative values of bBIC represent superior fit of the DSTP model. These frequency plots show that the SSP was slightly superior across participants for Experiments 1 and 2, but the DSTP was superior across participants in Experiment 3.

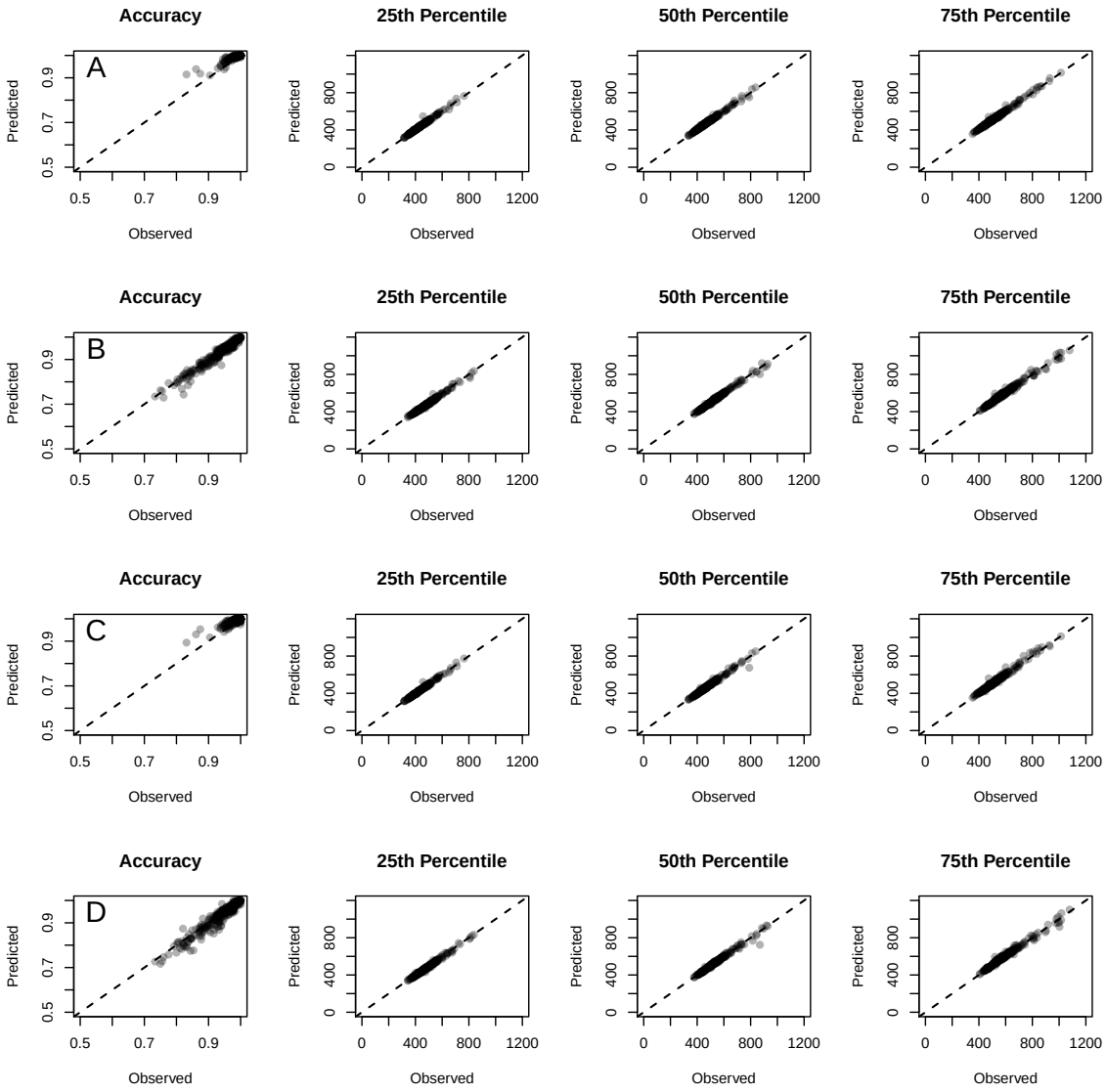

Figure D1. QQ-plots assessing goodness of fit for all models in Experiment 1. Row A: DSTP model, congruent data. Row B: DSTP model, incongruent data. Row C: SSP model, congruent data. Row D: SSP model, incongruent data. The diagonal dashed line represents the theoretical perfect fit.

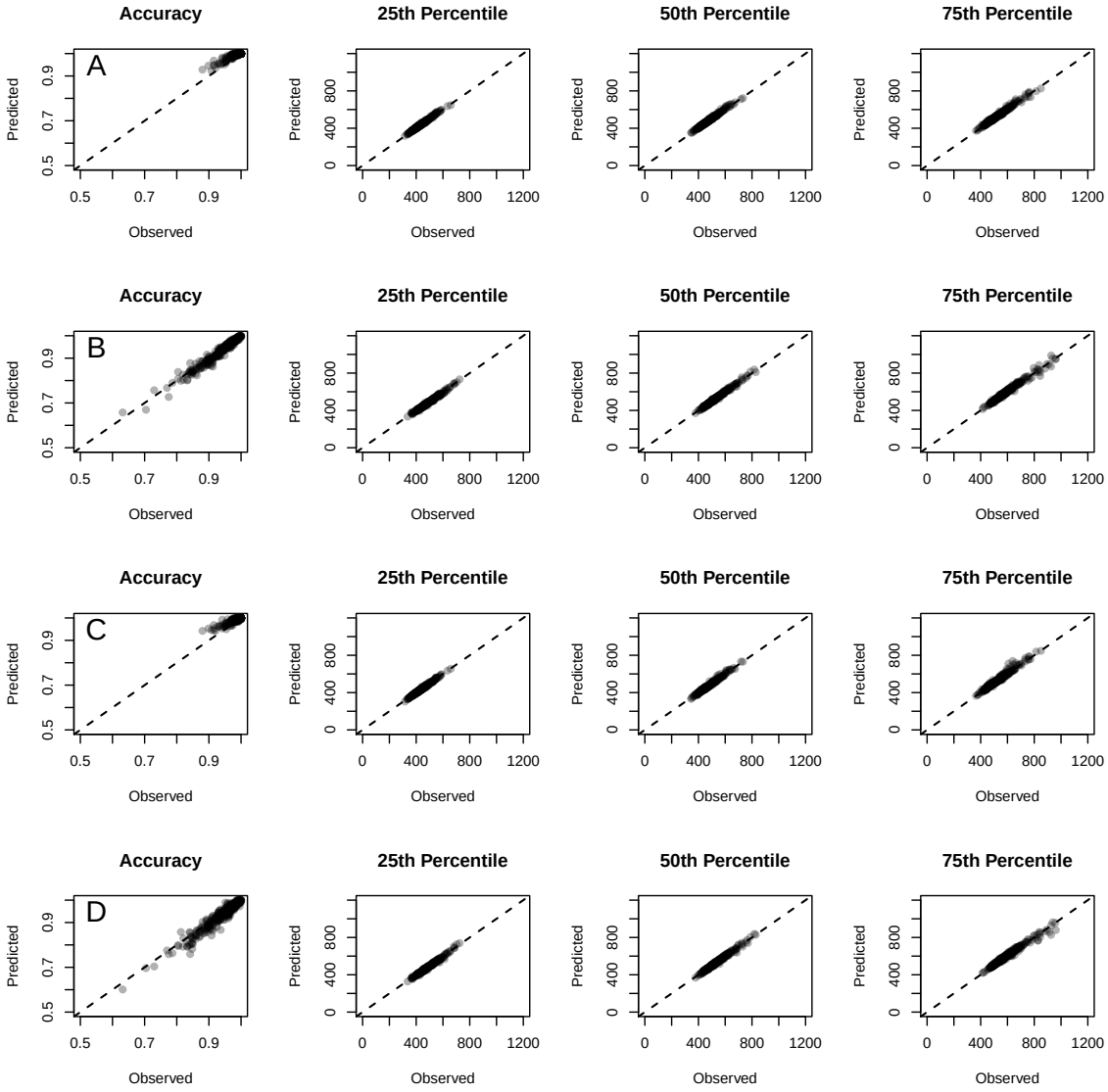

Figure D2. QQ-plots assessing goodness of fit for all models in Experiment 2. Row A: DSTP model, congruent data. Row B: DSTP model, incongruent data. Row C: SSP model, congruent data. Row D: SSP model, incongruent data. The diagonal dashed line represents the theoretical perfect fit.

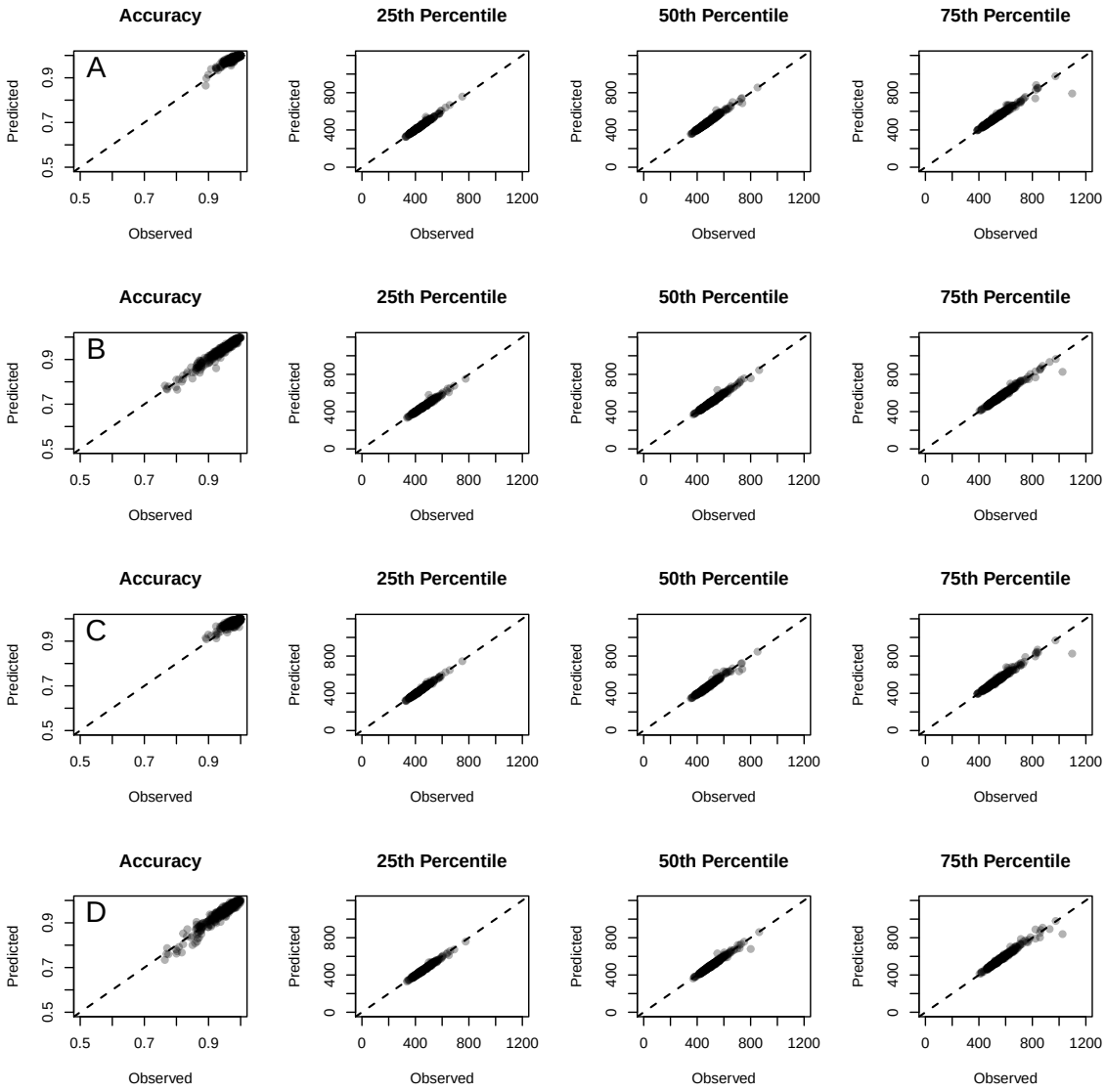

Figure D3. QQ-plots assessing goodness of fit for all models in Experiment 3. Row A: DSTP model, congruent data. Row B: DSTP model, incongruent data. Row C: SSP model, congruent data. Row D: SSP model, incongruent data. The diagonal dashed line represents the theoretical perfect fit.

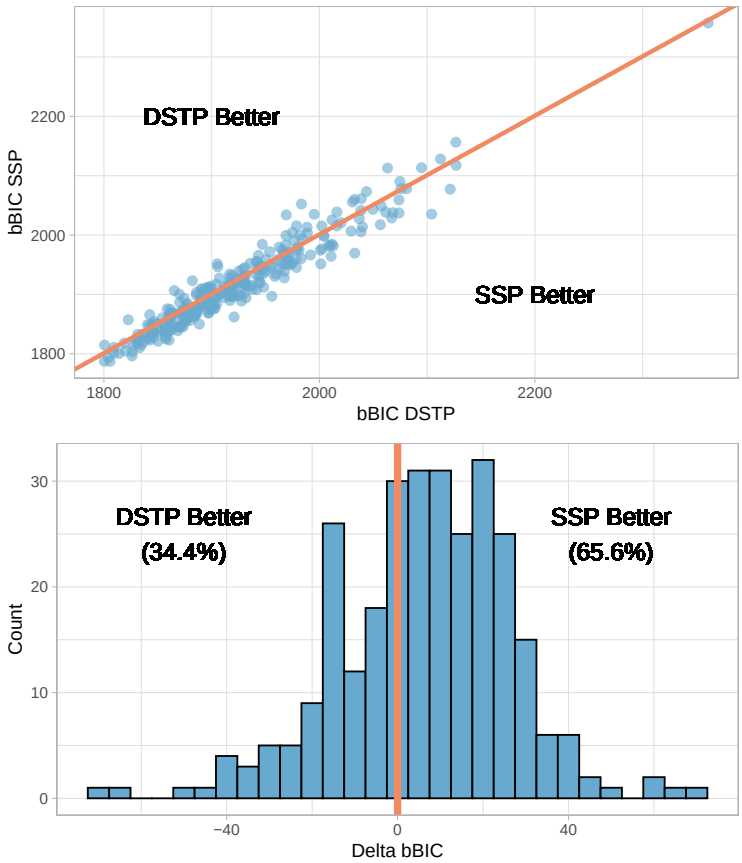

Figure D4. Representation of the assessment of model superiority across all participants in Experiment 1. Upper Panel: bBIC scores for the DSTP fit plotted against the bBIC scores for the SSP fit, across all participants. The diagonal line represents equivalence between both models. Data points below the diagonal represent participants for whom the SSP model fit their data than the DSTP model; the data points above the diagonal represent participants for whom the DSTP provided the superior fit. Lower Panel: The difference between bBIC scores for each model across participants (delta bBIC = bBIC[DSPT] – bBIC[SSP]). Positive values of delta bBIC indicate the SSP model is superior; negative values indicate superiority of the DSTP model. Percentages indicate the proportion of participants whose data were fit better by the respective model.

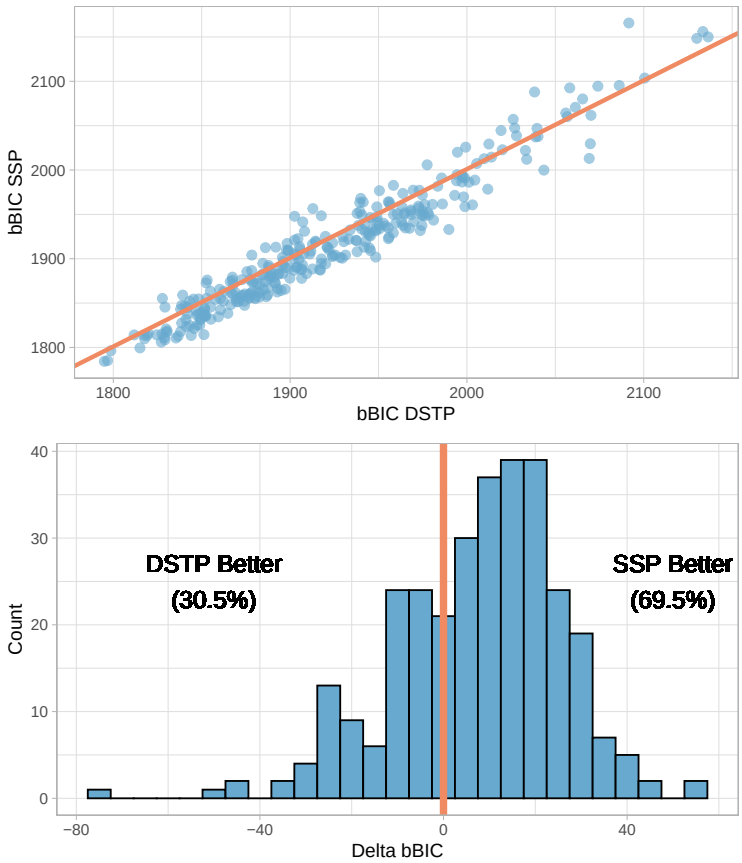

Figure D5. Representation of the assessment of model superiority across all participants in Experiment 2. Upper Panel: bBIC scores for the DSTP fit plotted against the bBIC scores for the SSP fit, across all participants. The diagonal line represents equivalence between both models. Data points below the diagonal represent participants for whom the SSP model fit their data than the DSTP model; the data points above the diagonal represent participants for whom the DSTP provided the superior fit. Lower Panel: The difference between bBIC scores for each model across participants (delta bBIC = bBIC[DSPT] – bBIC[SSP]). Positive values of delta bBIC indicate the SSP model is superior; negative values indicate superiority of the DSTP model. Percentages indicate the proportion of participants whose data were fit better by the respective model.

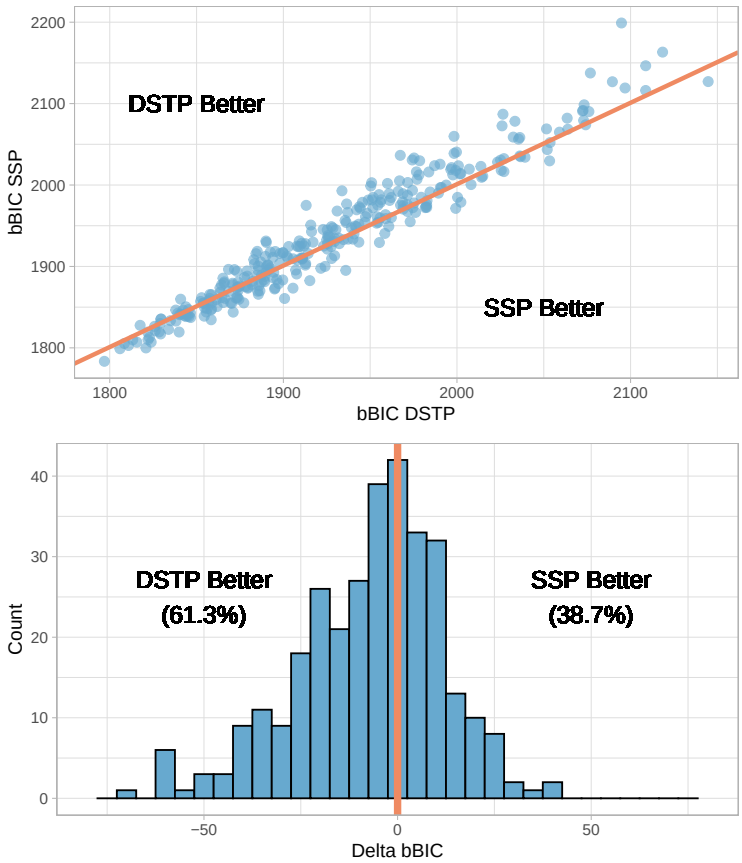

Figure D6. Representation of the assessment of model superiority across all participants in Experiment 3. Upper Panel: bBIC scores for the DSTP fit plotted against the bBIC scores for the SSP fit, across all participants. The diagonal line represents equivalence between both models. Data points below the diagonal represent participants for whom the SSP model fit their data than the DSTP model; the data points above the diagonal represent participants for whom the DSTP provided the superior fit. Lower Panel: The difference between bBIC scores for each model across participants (delta bBIC = bBIC[DSPT] – bBIC[SSP]). Positive values of delta bBIC indicate the SSP model is superior; negative values indicate superiority of the DSTP model. Percentages indicate the proportion of participants whose data were fit better by the respective model.

Appendix E
Model Regression Plots

This section presents plots of the Bayesian regressions predicting DSTP and SSP model parameters from QIDS and SHPS scores for Experiment 1–3.

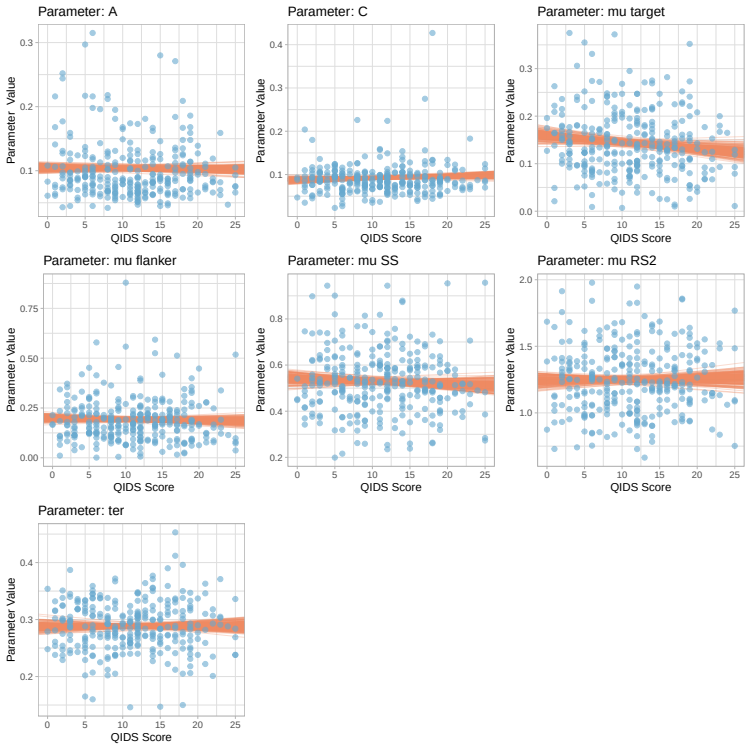

Figure E1. DSTP model parameters predicted from QIDS scores in Experiment 1. Points represent individual participant data; lines represent 200 draws from the posterior distribution of the Bayesian regression model, showing credible estimates of the linear relationship.

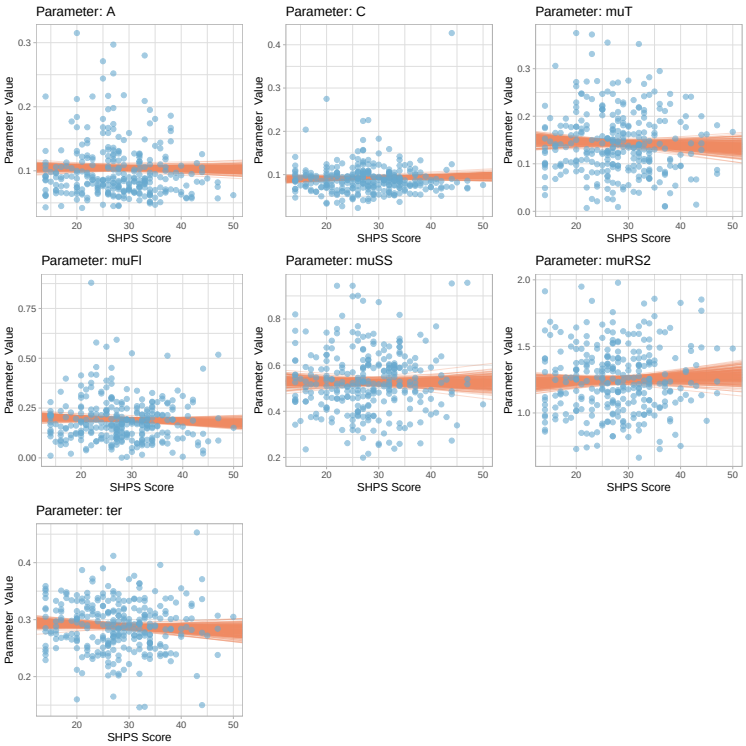

Figure E2. DSTP model parameters predicted from SHPS scores in Experiment 1. Points represent individual participant data; lines represent 200 draws from the posterior distribution of the Bayesian regression model, showing credible estimates of the linear relationship.

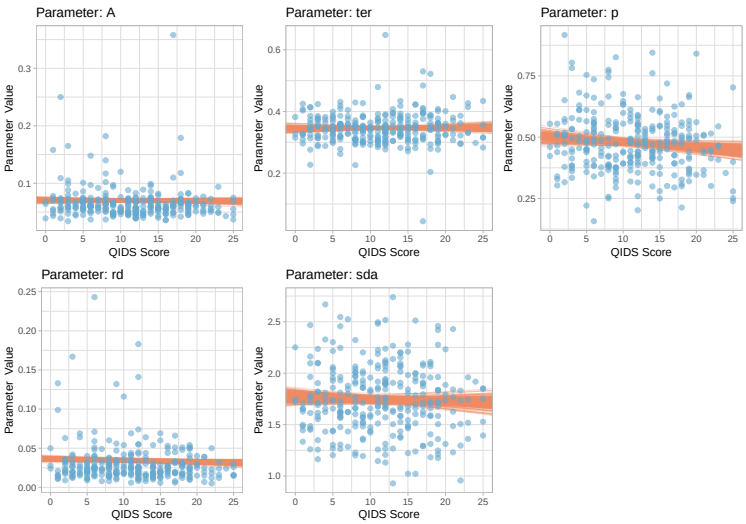

Figure E3. SSP model parameters predicted from QIDS scores in Experiment 1. Points represent individual participant data; lines represent 200 draws from the posterior distribution of the Bayesian regression model, showing credible estimates of the linear relationship.

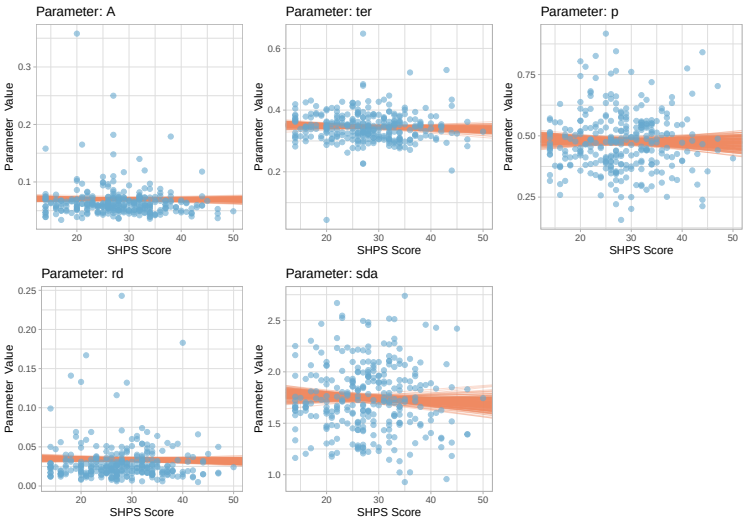

Figure E4. SSP model parameters predicted from SHPS scores in Experiment 1. Points represent individual participant data; lines represent 200 draws from the posterior distribution of the Bayesian regression model, showing credible estimates of the linear relationship.

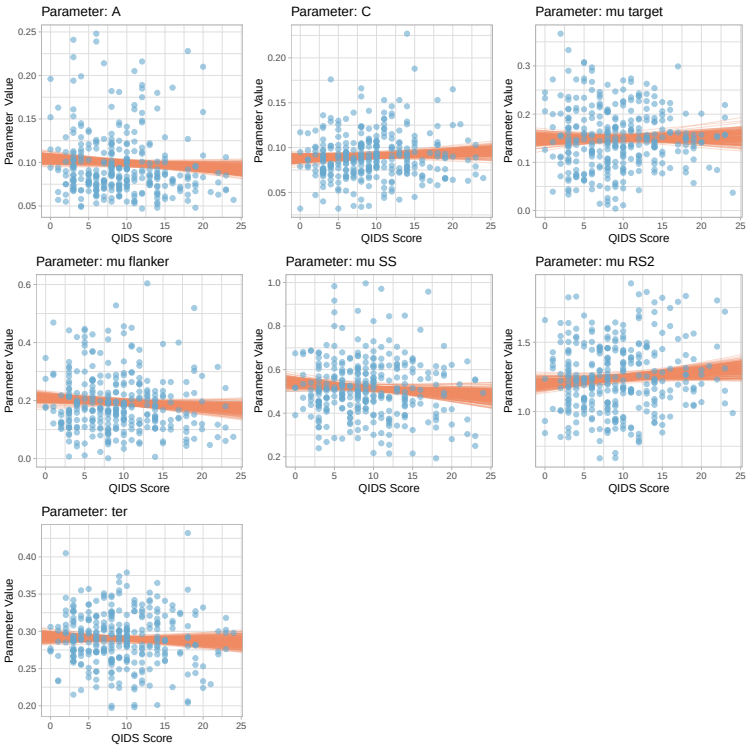

Figure E5. DSTP model parameters predicted from QIDS scores in Experiment 2. Points represent individual participant data; lines represent 200 draws from the posterior distribution of the Bayesian regression model, showing credible estimates of the linear relationship.

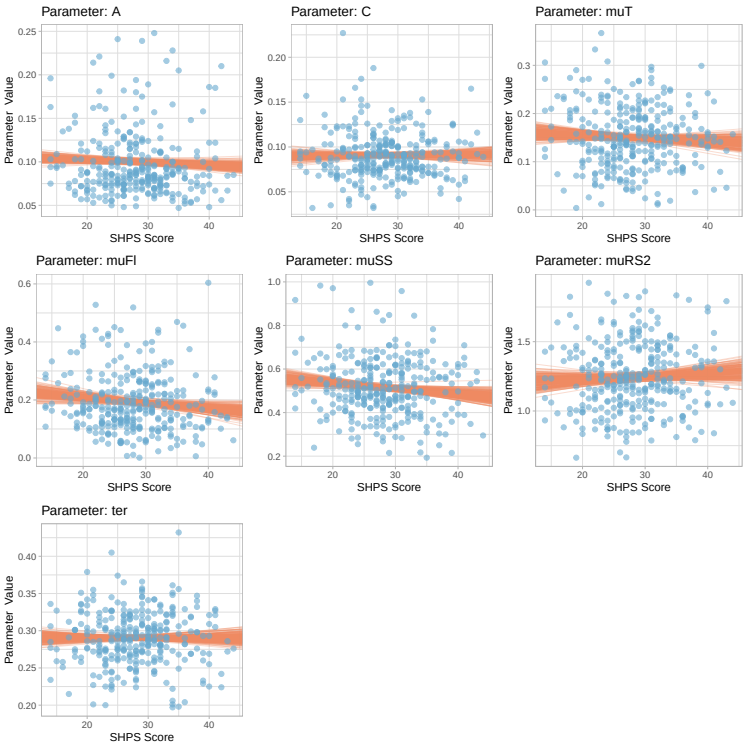

Figure E6. DSTP model parameters predicted from SHPS scores in Experiment 2. Points represent individual participant data; lines represent 200 draws from the posterior distribution of the Bayesian regression model, showing credible estimates of the linear relationship.

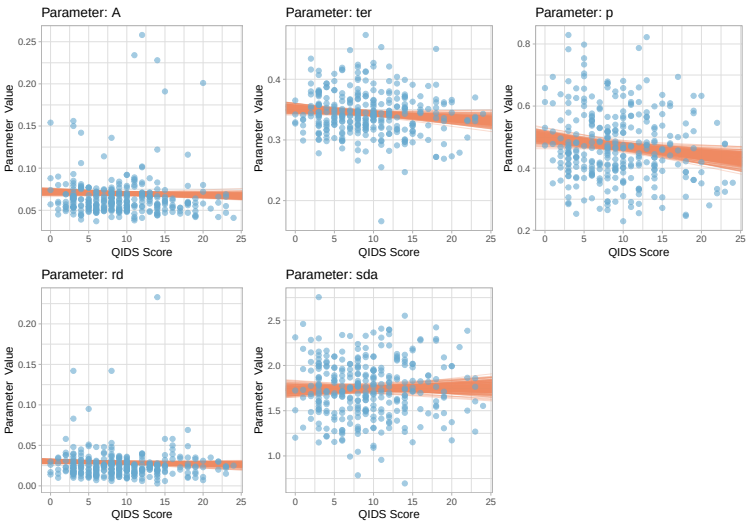

Figure E7. SSP model parameters predicted from QIDS scores in Experiment 2. Points represent individual participant data; lines represent 200 draws from the posterior distribution of the Bayesian regression model, showing credible estimates of the linear relationship.

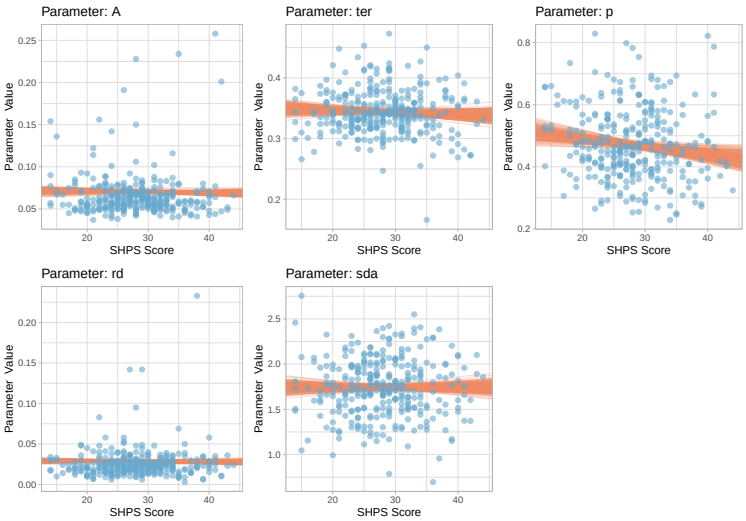

Figure E8. SSP model parameters predicted from SHPS scores in Experiment 2. Points represent individual participant data; lines represent 200 draws from the posterior distribution of the Bayesian regression model, showing credible estimates of the linear relationship.

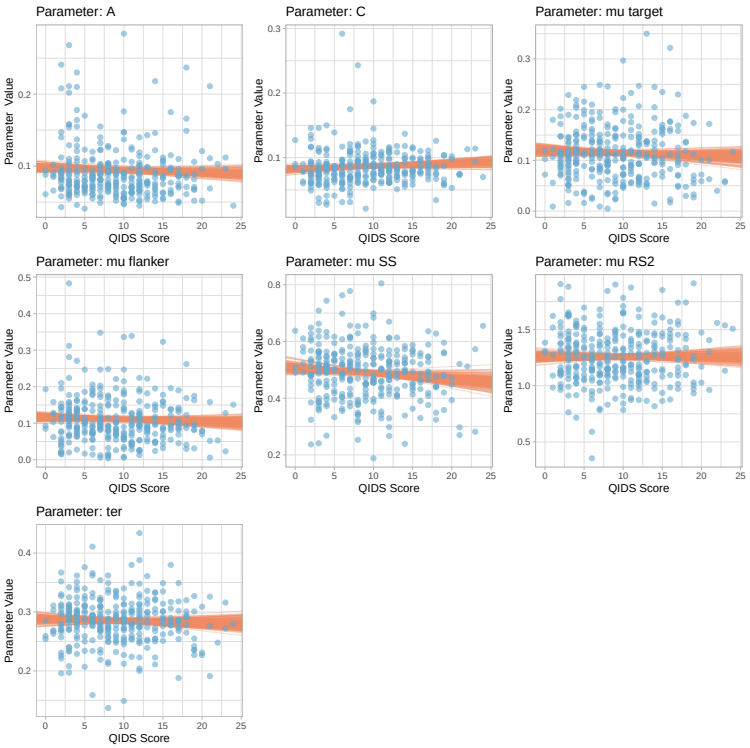

Figure E9. DSTP model parameters predicted from QIDS scores in Experiment 3. Points represent individual participant data; lines represent 200 draws from the posterior distribution of the Bayesian regression model, showing credible estimates of the linear relationship.

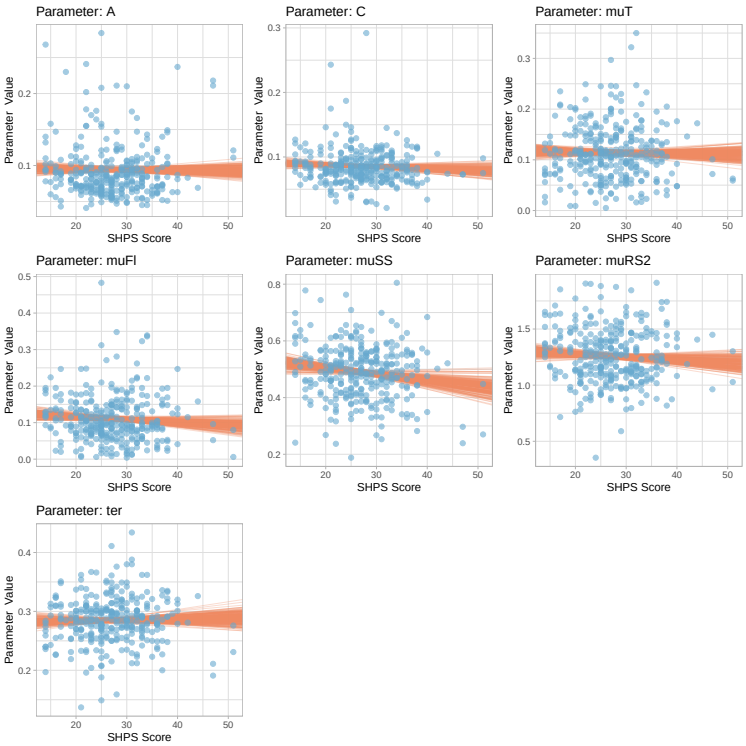

Figure E10. DSTP model parameters predicted from SHPS scores in Experiment 3. Points represent individual participant data; lines represent 200 draws from the posterior distribution of the Bayesian regression model, showing credible estimates of the linear relationship.

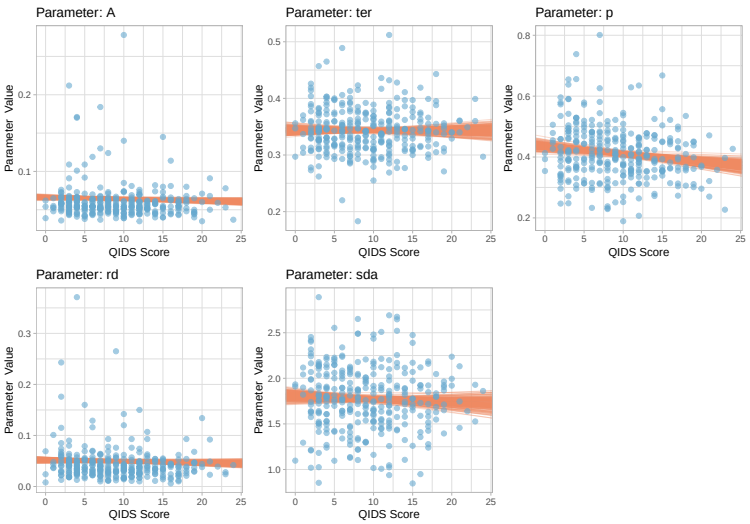

Figure E11. SSP model parameters predicted from QIDS scores in Experiment 3. Points represent individual participant data; lines represent 200 draws from the posterior distribution of the Bayesian regression model, showing credible estimates of the linear relationship.

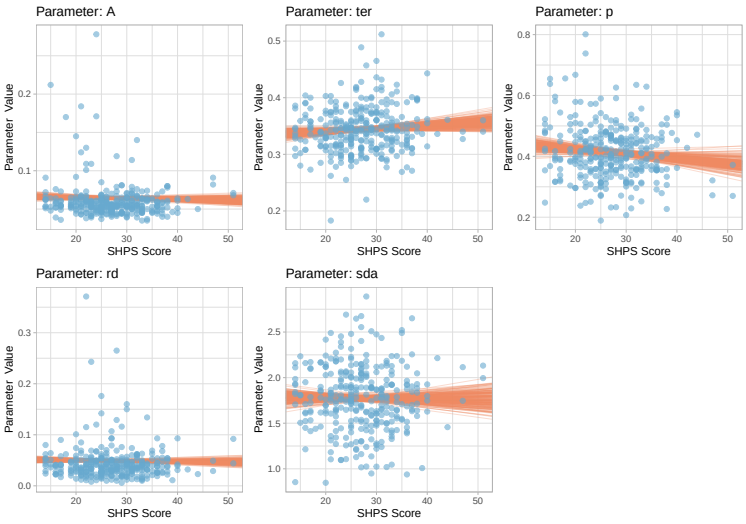

Figure E12. SSP model parameters predicted from SHPS scores in Experiment 3. Points represent individual participant data; lines represent 200 draws from the posterior distribution of the Bayesian regression model, showing credible estimates of the linear relationship.

Appendix F
Extreme QIDS Sub-Analysis

In this section, we provide a between-groups analysis on our dependent variables by grouping participants who scored 14 or above on the QIDS into a "high-QIDS" group, and those who scored below 8 into a "low-QIDS" group. We chose these QIDS scores as grouping cutoffs as they represent the values used for inclusion in the depressed group and the control group, respectively, in the study of Dillon et al. (2015). In our experiments, there were 109, 67, and 70 who were classified as high-QIDS in Experiments 1–3 respectively; for the low-QIDS groups, we had 88, 122, and 137 participants in Experiments 1–3 respectively.

We first provide an analysis on the behavioural data (i.e., RTs and accuracy) before analysing the model parameters. All analyses utilised Bayesian linear regressions with the respective DV as the outcome variable, and "QIDS group" as a categorical predictor. Regression coefficients for the QIDS-group predictor report the deviation of the low-QIDS group from the high-QIDS group (i.e., positive Beta values represent higher scores for the low-QIDS group in comparison to the high-QIDS group.

Behavioural Data

Density distributions of the outcome variables for the behavioural data for Experiments 1–3 can be seen in Figures F1–F3. The regression parameter values are shown in Table F1.

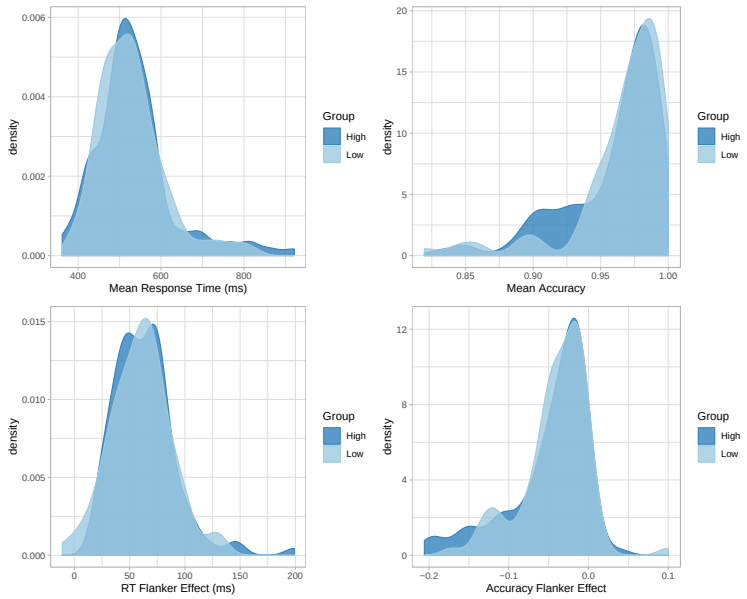

Figure F1. Density distributions of Experiment 1 data split by high QIDS scorers (above 14) and low QIDS scorers (below 8) for the dependent variables mean response time (in milliseconds, ms), mean proportion accuracy, flanker effect (response time, in ms), and flanker effect in accuracy (proportion).

Each plot shows the effect of QIDS grouping on mean response time, mean accuracy, the flanker effect in RT, and the flanker effect in accuracy. No differences were evidence in

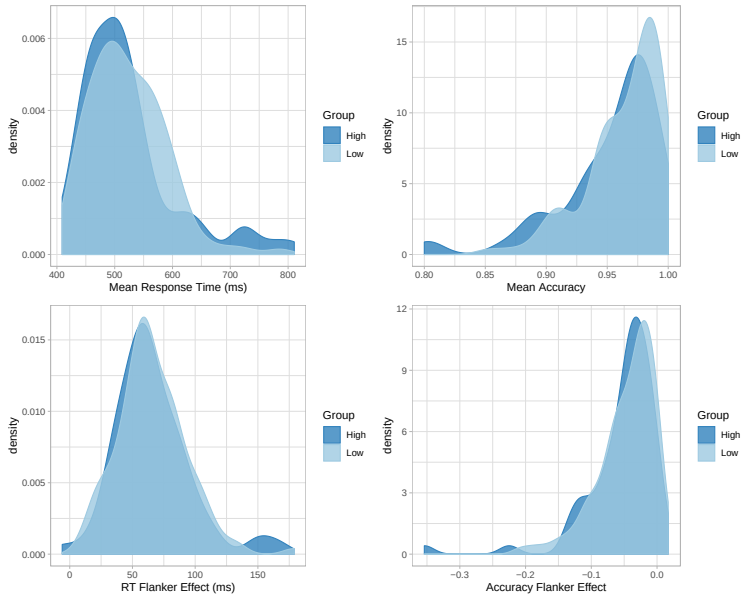

Figure F2. Density distributions of Experiment 2 data split by high QIDS scorers (above 14) and low QIDS scorers (below 8) for the dependent variables mean response time (in milliseconds, ms), mean proportion accuracy, flanker effect (response time, in ms), and flanker effect in accuracy (proportion).

any of the Experiments for the behavioural data.

Although there were no differences at the mean level, it is important to remember that the models are fit to the distributional data (the CDF and the CAF data). Visual inspection of these data suggest that there may be group differences that the models could explain. The cumulative distribution frequency plots of correct RT and the conditional accuracy functions for Experiments 1–3 are shown in Figure F4. There were no consistent differences between groups in the CDF plots; however, for the CAF plots, high-QIDS groups showed larger flanker effects in accuracy for the fastest RT bin, generally caused by poorer accuracy in the incongruent condition for high-QIDS scorers compared to low-QIDS scorers. This was generally true only for the fastest RT bin, with the exception of Experiment 3 where high-QIDS scorers generally had poorer accuracy throughout the whole RT distribution for incongruent trials.

DSTP Model Parameters

Density distributions of group differences on parameter estimates from the DSTP model are shown in Figures F5–F7. The parameter values for the Bayesian regressions are shown in Table F1. There were no consistent effects of QIDS score on any DSTP model parameter, with the exception of the μ_{SS} parameter in Experiment 3, which was lower in the high-QIDS group compared to the low-QIDS group. This reduction suggests that high-QIDS participants were slower to select the central target for further processing, thus delaying the shift from the first phase of response selection to the more-selective second phase of response selection. However, this effect was not evident in any of the other experiments, so

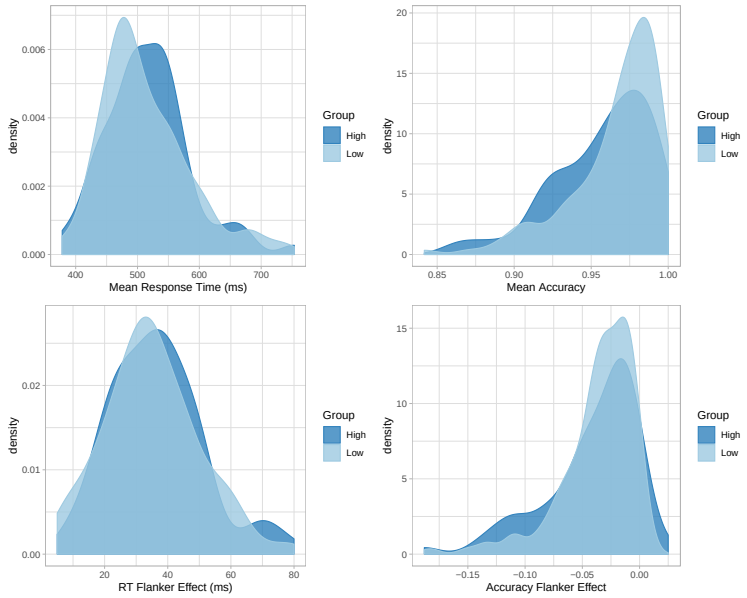

Figure F3. Density distributions of Experiment 3 data split by high QIDS scorers (above 14) and low QIDS scorers (below 8) for the dependent variables mean response time (in milliseconds, ms), mean proportion accuracy, flanker effect (response time, in ms), and flanker effect in accuracy (proportion).

we do not place much weight on this finding.

SSP Model Parameters

Density distributions of group differences on parameter estimates from the SSP model are shown in Figures F8–F10. The parameter values for the Bayesian regressions are shown in Table F1.

Replicating the findings from the regressions reported in the main body of the paper, estimates of model parameter p were lower in the high-QIDS group than the low-QIDS group, although the 95%CI for the regression predictor coefficient in Experiment 1 included zero. This suggests that high-QIDS participants had weaker perceptual representations of the stimulus than those in the low-QIDS group.

The *ter* parameter was also lower in the high-QIDS group than the low-QIDS group for Experiment 2, but this did not replicate in either of the other experiments, so again we do not place much weight on this finding.

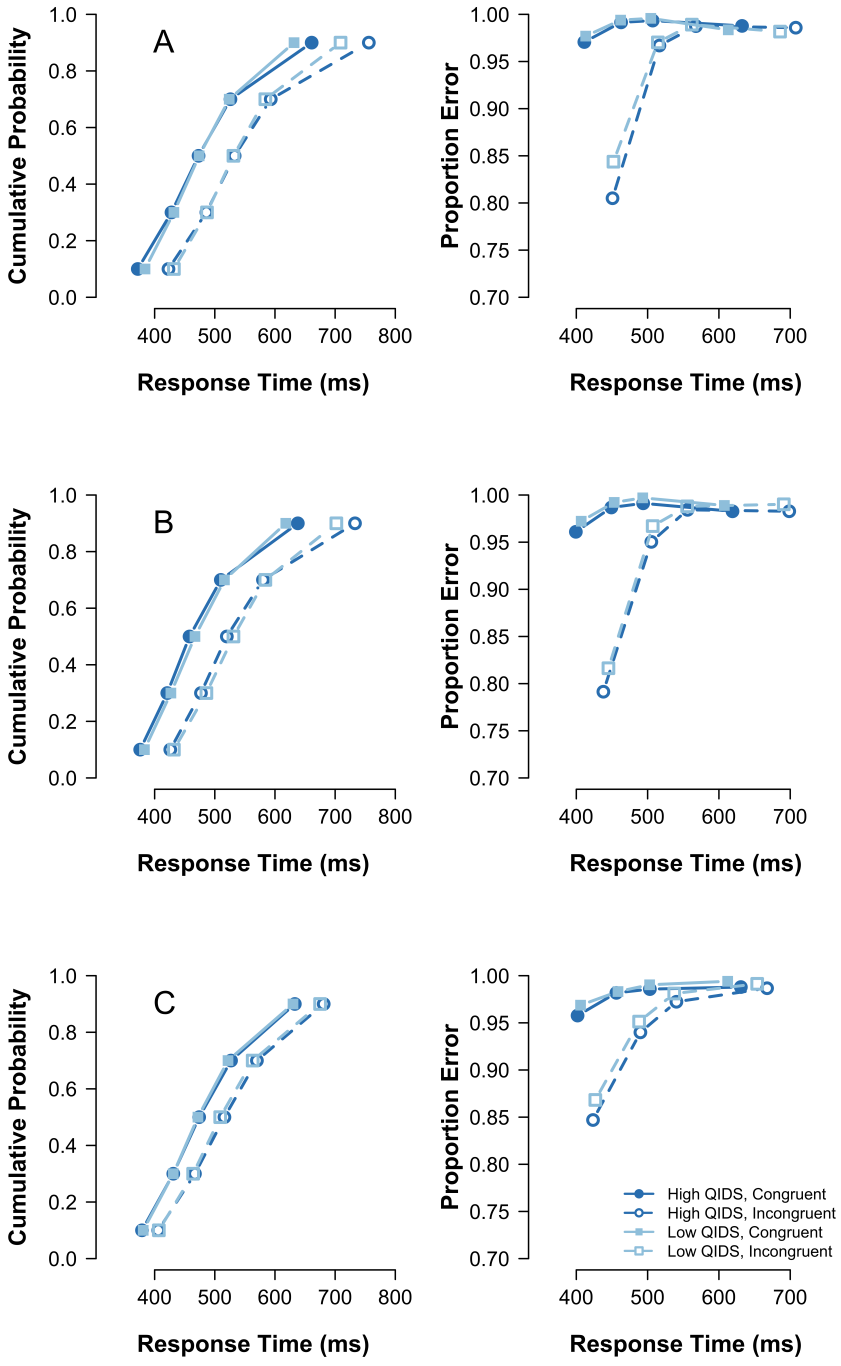

Figure F4. CDFs and CAFs for High and Low QIDS scoring participants. A–C plots Experiments 1–3.)

Table F1

Regression coefficients for the series of Bayesian regressions predicting dependent variable scores (DV) from the categorical predictor QIDS-Group across all Experiments. The values represent the mean estimate of the posterior distribution for each coefficient, together with their 95% credible interval in square parentheses. Entries in bold face represent regression predictors whose credible interval does not include zero (indicating the presence of an effect).

		Experiment 1		Experiment 2		Experiment 3	
Source	DV	$\beta_{Intercept}$	β_{Group}	$\beta_{Intercept}$	β_{Group}	$\beta_{Intercept}$	β_{Group}
Behavioural	Mean RT	529.31 [515.21, 544.17]	0.58 [-19.42, 20.56]	515.77 [501.55, 530.69]	8.01 [-8.24, 24.38]	516.65 [501.83, 531.76]	-5.64 [-22.93, 11.66]
	Mean Acc.	0.958 [0.953, 0.963]	0.003 [-0.001, 0.004]	0.956 [0.950, 0.962]	0.002 [-0.004, 0.008]	0.960 [0.955, 0.965]	0.002 [-0.002, 0.007]
	Fl. RT	63.22 [57.89, 68.38]	-3.11 [-10.67, 4.54]	65.72 [58.77, 72.60]	-0.36 [-8.56, 8.10]	36.46 [32.93, 40.07]	-1.52 [-5.90, 2.85]
	Fl. Acc	-0.05 [-0.06, -0.04]	0.01 [-0.01, 0.02]	-0.06 [-0.06, -0.05]	0.004 [-0.004, 0.012]	-0.04 [-0.05, -0.03]	-0.003 [-0.010. 0.004]
DSTP	A	0.1067 [0.0999. 0.1137]	0.0019 [-0.0063, 0.0102]	0.0953 [0.0888, 0.1017]	0.0064 [-0.0003, 0.0135]	0.0957 [0.0891, 0.1022]	0.0036 [-0.0030, 0.0108]
	C	0.0968 [0.0908, 0.1031]	-0.0070 [-0.0156, 0.0017]	0.0928 [0.0872, 0.0985]	-0.0054 [-0.0122, 0.0015]	0.0886 [0.0822, 0.0945]	-0.0065 [-0.0136, 0.0007]
	mu_T	0.1365 [0.1243, 0.1485]	0.0127 [-0.0051, 0.0305]	0.1588 [0.1420, 0.1747]	-0.0087 [-0.0281, 0.0122]	0.1115 [0.0991, 0.1239]	0.0058 [-0.0086, 0.0208]
	mu_Fl	0.1900 [0.1719, 0.2087]	0.0074 [-0.0173, 0.0312]	0.1746 [0.1538, 0.1960]	0.00246 [0.0003, 0.0502]	0.1101 [0.0964, 0.1236]	0.0077 [-0.0078, 0.0240]
	mu_SS	0.5190 [0.4940, 0.5446]	0.0146 [-0.0229, 0.0526]	0.4941 [0.4633, 0.5248]	0.0262 [-0.0123, 0.0656]	0.4749 [0.4525, 0.4968]	**0.0285 [0.0016, 0.0561]**
	mu_RS2	1.2638 [1.2166, 1.3134]	-0.0227 [-0.0933, 0.0495]	1.2779 [1.2225, 1.3326]	-0.0462 [-0.1142, 0.0220]	1.2869 [1.2257, 1.3480]	-0.0273 [-0.1039, 0.0462]
	ter	0.2902 [0.2812, 0.2986]	0.0003 [-0.0131, 0.0138]	0.2893 [0.2809, 0.2977]	0.0035 [-0.0074, 0.0143]	0.2822 [0.2732, 0.2914]	0.0056 [-0.0054, 0.0163]
SSP	a	0.0723 [0.0682, 0.0767]	0.0012 [-0.0038, 0.0062]	0.0683 [0.0645, 0.0722]	0.0019 [-0.0021, 0.0061]	0.0628 [0.0591, 0.0665]	0.0025 [-0.0011, 0.0064]
	ter	0.3484 [0.3391, 0.3578]	-0.0020 [-0.0169, 0.0123]	0.3352 [0.3271, 0.3437]	**0.0012 [0.0020, 0.0223]**	0.3460 [0.3370, 0.3553]	-0.0011 [-0.0119, 0.0101
	p	0.4676 [0.446, 0.4915]	0.0277 [-0.0065, 0.0604]	0.4485 [0.4227, 0.4743]	**0.0346 [0.0028, 0.0655]**	0.4022 [0.3806, 0.4229]	**0.0311 [0.0055, 0.0568**
	rd	0.0321 [0.0289, 0.0353]	0.0026 [-0.0008, 0.0059]	0.0295 [0.0262, 0.0327]	0.0018 [-0.0017, 0.0052]	0.0475 [0.0420, 0.0531]	0.0049 [-0.0006, 0.0108]
	sda	1.7232 [1.6599, 1.7836]	0.0251 [-0.0663, 0.1152]	1.7633 [1.6847, 1.8435]	1.7633 [1.6847, 1.8435]	1.7380 [1.6576, 1.8178]	0.0559 [-0.0401, 0.1513]

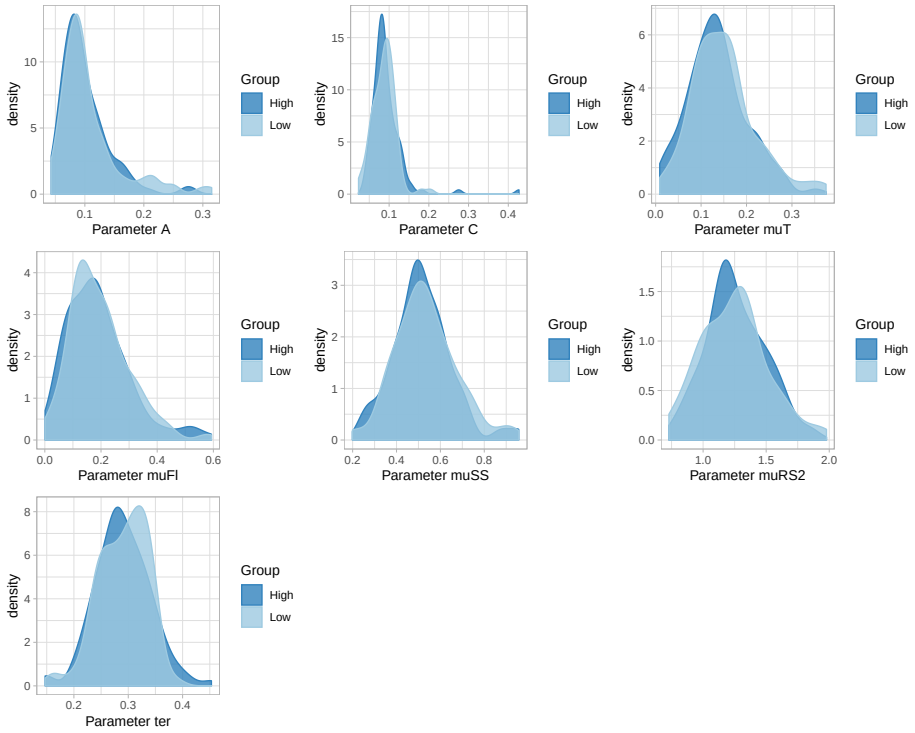

Figure F5. Density distributions of Experiment 1 data split by high QIDS scorers (above 14) and low QIDS scorers (below 8) for the parameters of the DSTP model.

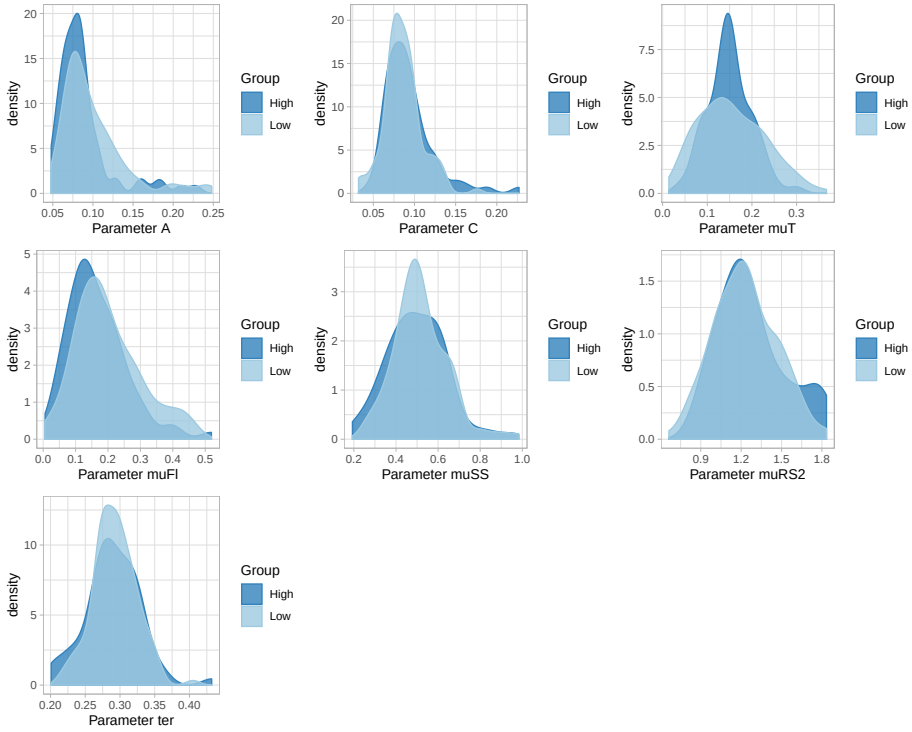

Figure F6. Density distributions of Experiment 2 data split by high QIDS scorers (above 14) and low QIDS scorers (below 8) for the parameters of the DSTP model.

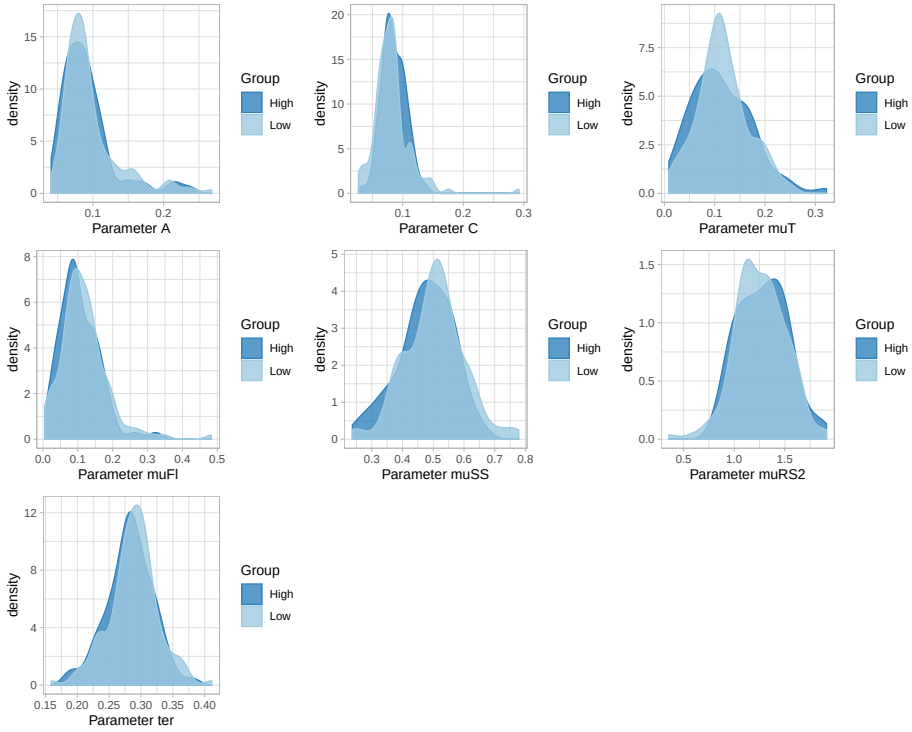

Figure F7. Density distributions of Experiment 3 data split by high QIDS scorers (above 14) and low QIDS scorers (below 8) for the parameters of the DSTP model.

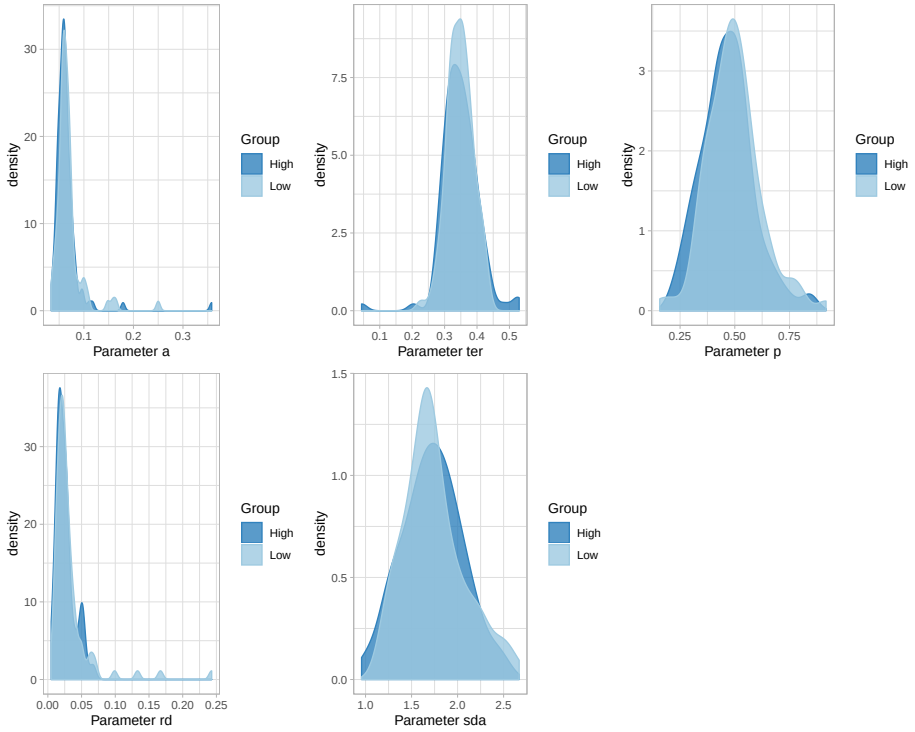

Figure F8. Density distributions of Experiment 1 data split by high QIDS scorers (above 14) and low QIDS scorers (below 8) for the parameters of the SSP model.

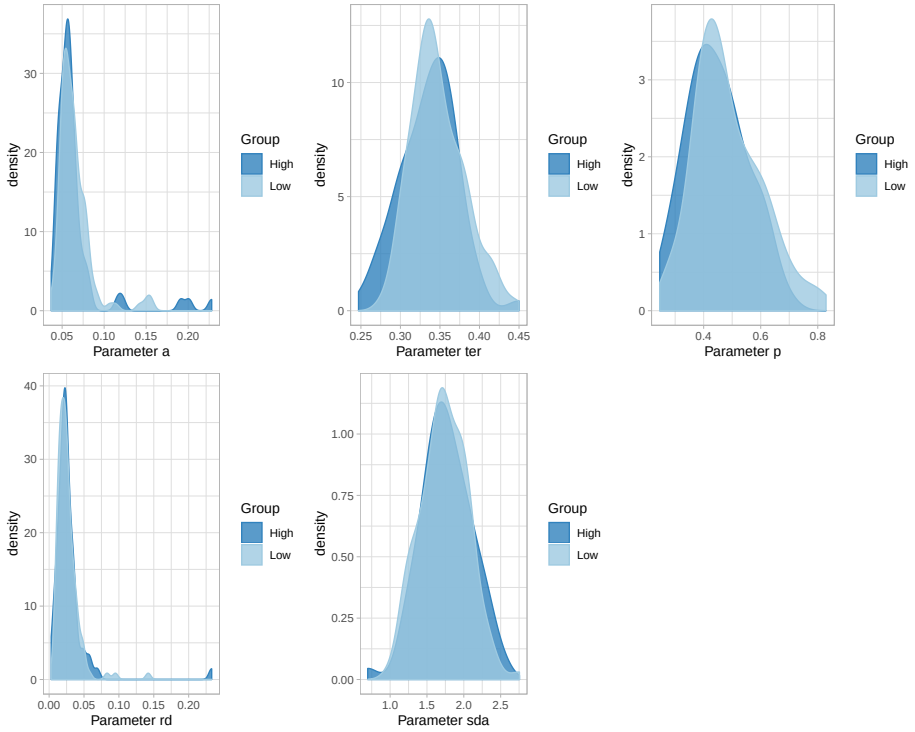

Figure F9. Density distributions of Experiment 2 data split by high QIDS scorers (above 14) and low QIDS scorers (below 8) for the parameters of the SSP model.

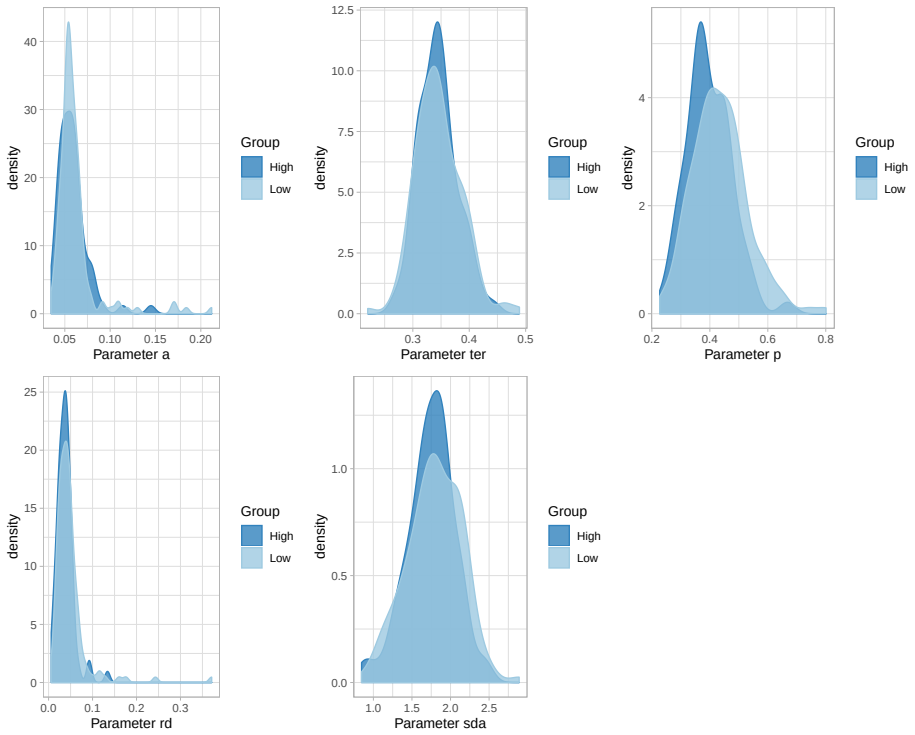

Figure F10. Density distributions of Experiment 3 data split by high QIDS scorers (above 14) and low QIDS scorers (below 8) for the parameters of the SSP model.

Appendix G
Depression Diagnosis Sub-Analysis

In this section we wished to identify those who declared a clinical diagnosis ("with depression") to those who declared they did not have a clinical diagnosis ("without depression") to observe whether there are group differences on the dependent variables QIDS scores, SHPS scores, response time flanker effect, and accuracy flanker effect, as well as of course the DSTP and SSP model parameters. In our Experiments, we had 30.95%, 23.15%, and 14.78% of participants who declared a depression diagnosis (Experiments 1–3 respectively).

Group differences on QIDS & SHPS

Before looking at group differences on the main dependent variabeles, we were interested in exploring whether those who declared a depression diagnosis scored higher on the QIDS and SHPS. Such a finding would provide reassurance that the self-declarations were truthful. The density distributions for these variables for both groups for all experiments are shown in Figures G1–G3. We modelled the data using a Bayesian regression, with the dependent variable predicted by Group (i.e., "with" vs. "without" depression). Regression coefficients for the Depression-Group report the deviation of the depressed group from the non-depressed group (i.e., positive Beta values represent higher scores for the non-depressed group).

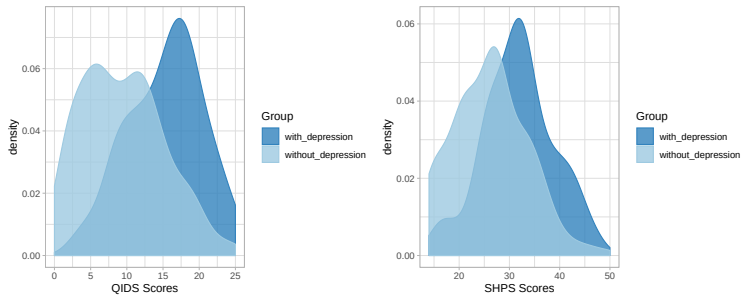

Figure G1. Density distributions of Experiment 1 data split by those declaring a depression diagnosis ("with depression") to those who declare no diagnosis of depression ("without depression") on the dependent variables QIDS scores and SHPS scores.

Experiment 1. For the QIDS questionnaire, those without depression demonstrated *lower* scores ($\beta_{Intercept}$ = 15.31 [14.16, 16.46], β_{Group} = -5.87 [-7.25, -4.46]). For the SHPS questionnaire, those without depression demonstrated lower scores ($\beta_{Intercept}$ = 31.76 [30.30, 33.23], β_{Group} = -5.57 [-7.36, -3.79]). These results suggest that the responses to both questionnaires were sensitive to depression diagnosis.

Experiment 2. For the QIDS questionnaire, those without depression demonstrated *lower* scores ($\beta_{Intercept}$ = 13.49 [12.49, 14.49], β_{Group} = −5.52 [−6.61, −4.46]). For the SHPS questionnaire, those without depression demonstrated lower scores ($\beta_{Intercept}$ = 31.95 [30.59, 33.31], β_{Group} = −5.11 [−6.66, −3.58]). These results suggest that the responses to both questionnaires were sensitive to depression diagnosis.

Experiment 3. For the QIDS questionnaire, those without depression demonstrated *lower* scores ($\beta_{Intercept}$ = 14.02 [13.06, 15.01], β_{Group} = −6.41 [−7.46, −5.39]).

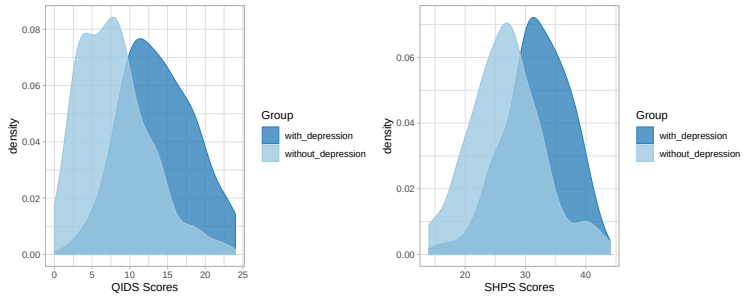

Figure G2. Density distributions of Experiment 2 data split by those declaring a depression diagnosis ("with depression") to those who declare no diagnosis of depression ("without depression") on the dependent variables QIDS scores and SHPS scores.

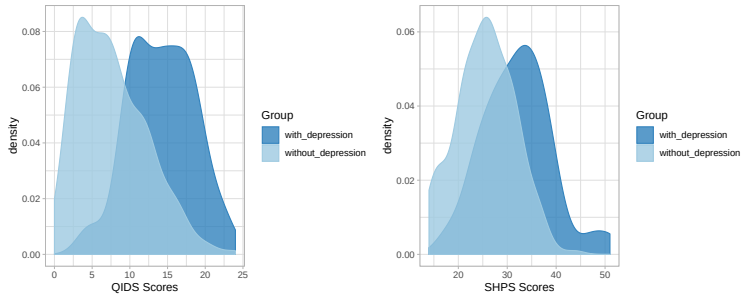

Figure G3. Density distributions of Experiment 3 data split by those declaring a depression diagnosis ("with depression") to those who declare no diagnosis of depression ("without depression") on the dependent variables QIDS scores and SHPS scores.

For the SHPS questionnaire, those without depression demonstrated lower scores ($\beta_{Intercept}$ = 32.06 [30.64, 33.46], β_{Group} = −6.49 [−8.11, −4.88]). These results suggest that the responses to both questionnaires were sensitive to depression diagnosis.

Behavioural Data

Density distributions of the outcome variables for the behavioural data for Experiments 1–3 can be seen in Figures G4–G6. The regression parameter values are shown in Table G1. Each plot shows the effect of Depression grouping on mean response time, mean accuracy, the flanker effect in RT, and the flanker effect in accuracy. No differences were evident.

Distributional data in the form of cumulative distribution functions and conditional accuracy functions for Experiments 1–3 can be found in Figure G7. There were no consistent differences between groups in the CDF plots; however, for the CAF plots, high-QIDS groups showed larger flanker effects in accuracy for the fastest RT bin in Experiment 1, generally caused by poorer accuracy in the incongruent condition for high-QIDS scorers compared to low-QIDS scorers. This was generally true only for the first experiment.

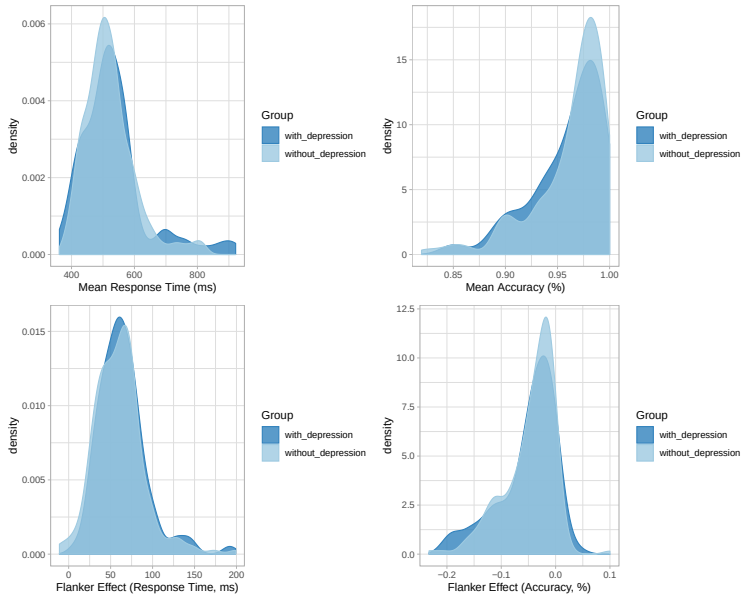

Figure G4. Density distributions of Experiment 1 data split by those declaring a depression diagnosis ("with depression") to those who declare no diagnosis of depression ("without depression") on the dependent variables Mean RT, flanker RT, mean accuracy, flanker accuracy.

DSTP Model Parameters

Density distributions of group differences on parameter estimates from the DSTP model are shown in Figures G8–G10. The parameter values for the Bayesian regressions are shown in Table G1. There were no consistent effects of depression on any DSTP model parameter, with the exception of the μ_{SS} parameter in Experiment 3, which was lower in the depressed group compared to the non-depressed group. This reduction suggests that depressed individuals were slower to select the central target for further processing, thus delaying the shift from the first phase of response selection to the more-selective second phase of response selection. However, this effect was not evident in any of the other experiments, so we do not place much weight on this finding.

SSP Model Parameters. Density distributions of group differences on parameter estimates from the SSP model are shown in Figures G11–G13. The parameter values for the Bayesian regressions are shown in Table C1. No SSP parameter differed according to depression grouping.

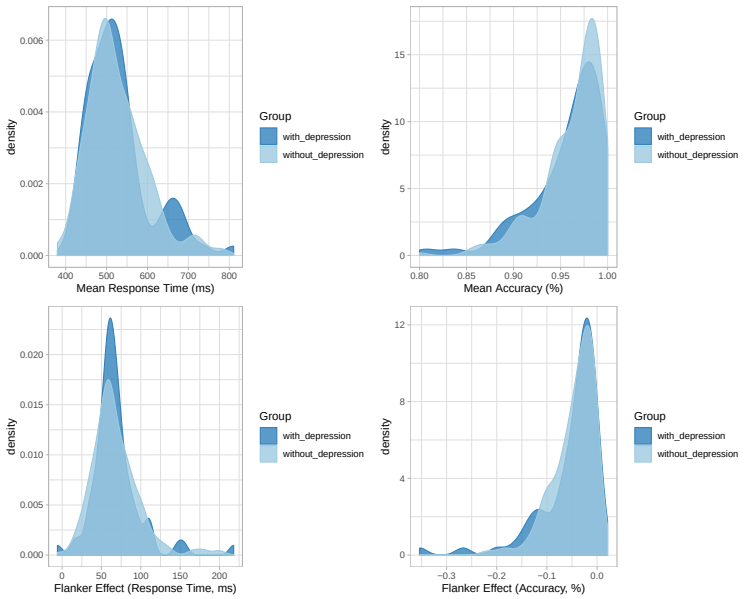

Figure G5. Density distributions of Experiment 2 data split by those declaring a depression diagnosis ("with depression") to those who declare no diagnosis of depression ("without depression") on the dependent variables Mean RT, flanker RT, mean accuracy, flanker accuracy.

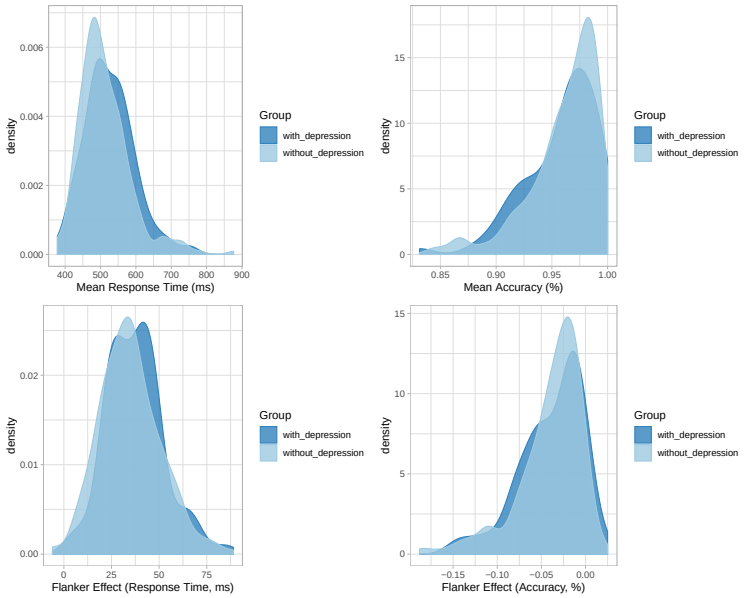

Figure G6. Density distributions of Experiment 3 data split by those declaring a depression diagnosis ("with depression") to those who declare no diagnosis of depression ("without depression") on the dependent variables Mean RT, flanker RT, mean accuracy, flanker accuracy.

Table G1

Regression coefficients for the series of Bayesian regressions predicting dependent variable scores (DV) from the categorical predictor depression diagnosis (with vs. without) across all Experiments. The values represent the mean estimate of the posterior distribution for each coefficient, together with their 95% credible interval in square parentheses. Entries in bold face represent regression predictors whose credible interval does not include zero (indicating the presence of an effect).

		Experiment 1		Experiment 2		Experiment 3	
Source	DV	$\beta_{Intercept}$	β_{Group}	$\beta_{Intercept}$	β_{Group}	$\beta_{Intercept}$	β_{Group}
Behavioural	Mean RT	521.30 [505.76, 536.68]	2.56 [-14.54, 20.00]	525.62 [510.52, 540.06]	-1.02 [-16.23, 15.21]	524.20 [509.53, 538.58]	-12.82 [28.19, 3.04]
	Mean Acc.	0.958 [0.954, 0.963]	0.001 [-0.003, 0.005]	0.959 [0.954, 0.964]	0.01 [-0.004, 0.004]	0.960 [0.956, 0.964]	-0.002 [-0.006, 0.003]
	Fl. RT	64.21 [58.14, 70.50]	-4.18 [-11.62, 3.26]	67.84 [60.75, 75.04]	-0.41 [-8.43, 7.73]	37.36 [33.75, 40.92]	-2.54 [-6.58, 1.50]
	Fl. Acc	-0.05 [-0.06, -0.04]	0.01 [-0.01, 0.02]	-0.05 [-0.06, -0.05]	0.003 [-0.005, 0.009]	-0.04 [-0.045, 0.033]	-0.003 [-0.001, 0.003]
DSTP	A	0.1026 [0.0962, 0.1090]	0.0014 [-0.0050, 0.0080]	0.0964 [0.0904, 0.1024]	0.0044 [-0.0014, 0.0106]	0.0955 [0.0901, 0.1009]	-0.0012 [-0.0065, 0.0045]
	C	0.0952 [0.0888, 0.1015]	-0.0037 [-0.0107, 0.0035]	0.0907 [0.0849, 0.0966]	0.0002 [-0.0064, 0.0068]	0.0892 [0.0835, 0.0948]	-0.0042 [-0.0105, 0.0021]
	mu_T	0.1403 [0.1270, 0.1536]	-0.0049 [-0.0101, 0.0205]	0.1516 [0.1359, 0.1662]	-0.0017 [-0.0186, 0.0161]	0.1098 [0.0989, 0.1211]	0.0062 [-0.0062, 0.0192
	mu_Fl	0.1906 [0.1714, 0.2097]	0.0021 [-0.0188, 0.0230]	0.1833 [0.1631, 0.2039]	0.0123 [-0.0095, 0.0346]	0.1082 [0.0956, 0.1210]	0.0036 [-0.0099, 0.0178]
	mu_SS	0.5159 [0.4884, 0.5426]	0.0170 [-0.0168, 0.0512]	0.5078 [0.4766, 0.5389]	0.0111 [-0.0257, 0.0472]	0.4685 [0.4462, 0.4904]	**0.0271 [0.0022, 0.0529]**
	mu_RS2	1.2504 [1.1979, 1.3023]	-0.0224 [-0.0637, 0.0607]	1.2372 [1.1807, 1.2948]	0.0084 [-0.0585, 0.0741]	1.2573 [1.2021, 1.3125]	0.0027 [-0.0632, 0.0660]
	ter	0.2927 [0.2834, 0.3020]	-0.0224 [-0.0637, 0.0607]	0.2976 [0.2889, 0.3061]	-0.0096 [-0.0193, 0.0004]	0.2802 [0.2709, 0.2892]	0.0064 [-0.0040, 0.0171]
SSP	a	0.0693 [0.0655, 0.0731]	0.0012 [-0.0023, 0.0051]	0.0691 [0.0656, 0.0726]	0.0015 [-0.0018, 0.0051]	0.0661 [0.0630, 0.0692]	-0.0022 [-0.0052, 0.0009]
	ter	0.3529 [0.3428, 0.3628]	-0.0105 [-0.0227, 0.0016]	0.3466 [0.3375, 0.3554]	-0.0031 [-0.0131, 0.0069]	0.3460 [0.3370, 0.3555]	-0.0028 [-0.0134, 0.0075]
	p	0.4688 [0.4449, 0.4922]	0.0136 [-0.0155, 0.0429]	0.4533 [0.4289, 0.4818]	0.0206 [-0.0083, 0.0495]	0.3970 [0.3771, 0.4171]	0.0206 [-0.0018, 0.0436]
	rd	0.0330 [0.0299, 0.0360]	0.0020 [-0.0009, 0.0051]	0.0283 [0.0256, 0.0310]	0.0006 [-0.0021, 0.0035]	0.0482 [0.0433, 0.0531]	0.0018 [-0.0028, 0.0070]
	sda	1.7372 [1.6690, 1.8066]	0.0121 [-0.0673, 0.0946]	1.7213 [1.6434, 1.7976]	0.0282 [-0.0573, 0.1142]	1.7621 [1.6833, 1.8408]	0.0165 [-0.0757, 0.1062]

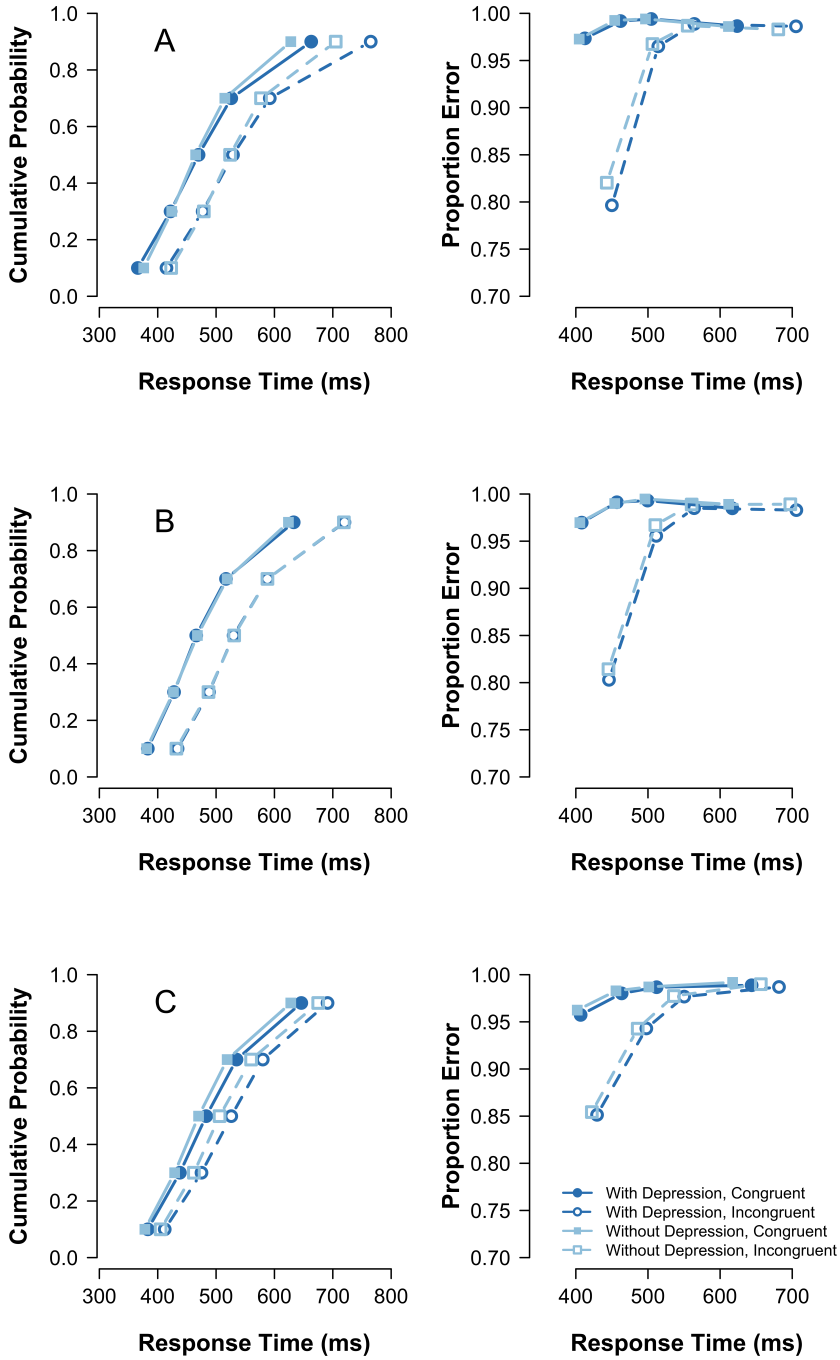

Figure G7. CDFs and CAFs for those participants self-declaring a diagnosis of depression, and those declaring no such diagnosis. A–C plots Experiments 1–3.)

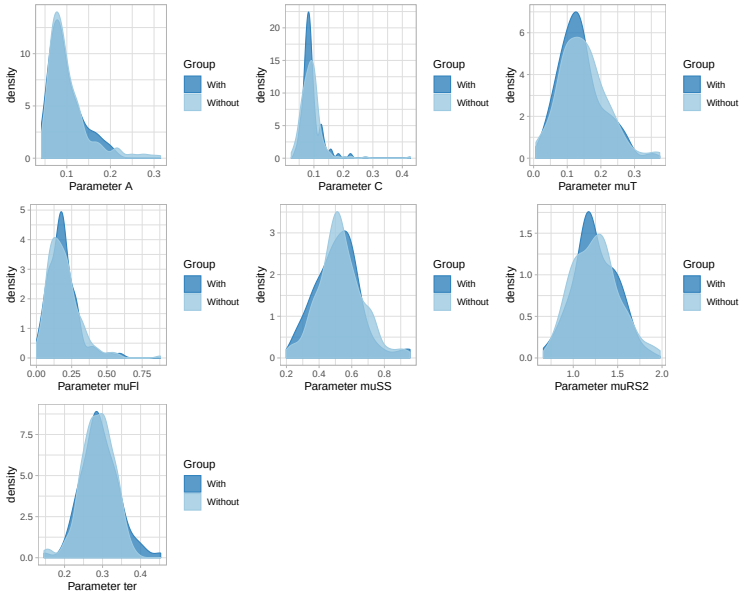

Figure G8. Density distributions of the DSTP model parameters in Experiment 1 split by those declaring a depression diagnosis ("with depression") to those who declare no diagnosis of depression ("without depression").

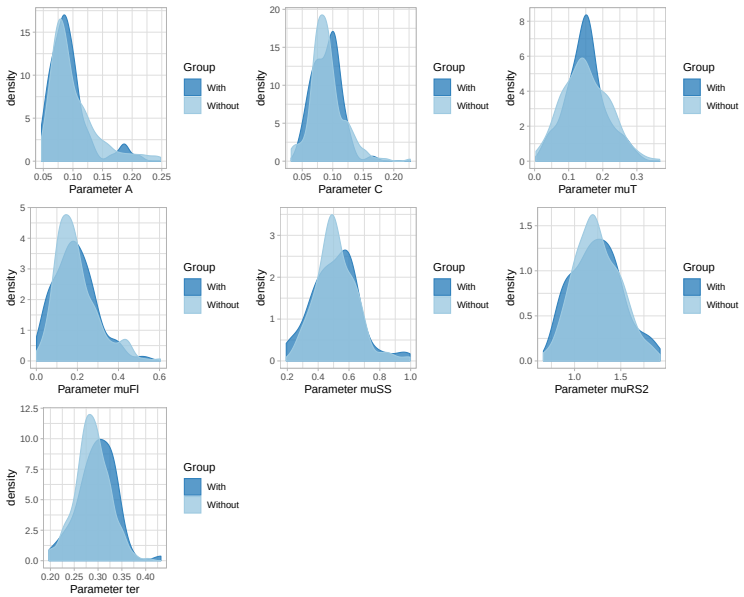

Figure G9. Density distributions of the DSTP model parameters in Experiment 2 split by those declaring a depression diagnosis ("with depression") to those who declare no diagnosis of depression ("without depression").

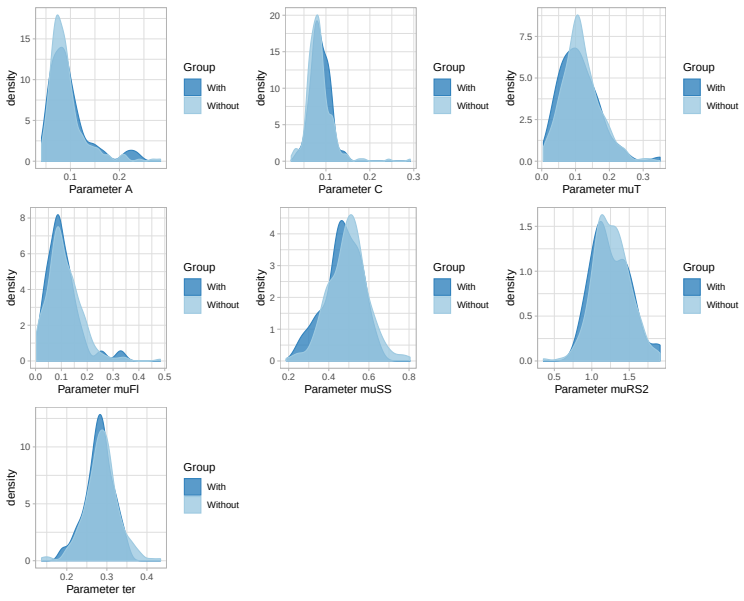

Figure G10. Density distributions of the DSTP model parameters in Experiment 3 split by those declaring a depression diagnosis ("with depression") to those who declare no diagnosis of depression ("without depression").

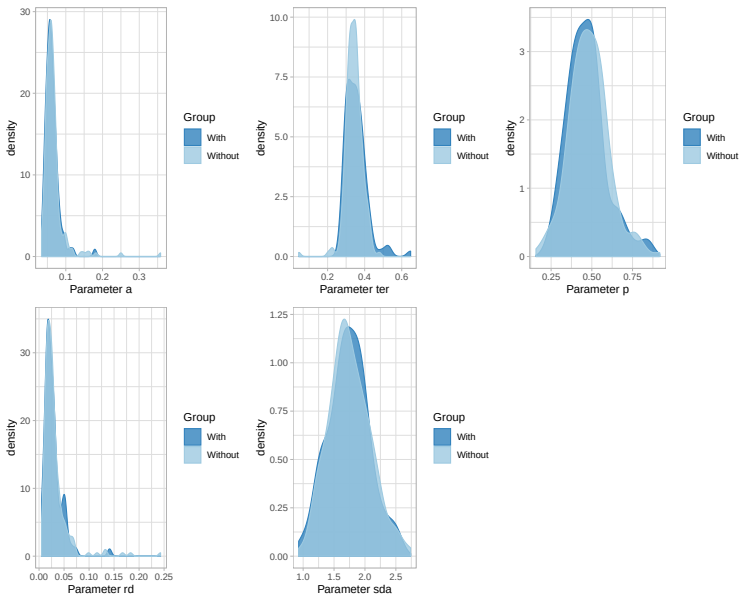

Figure G11. Density distributions of the SSP model parameters in Experiment 1 split by those declaring a depression diagnosis ("with depression") to those who declare no diagnosis of depression ("without depression").

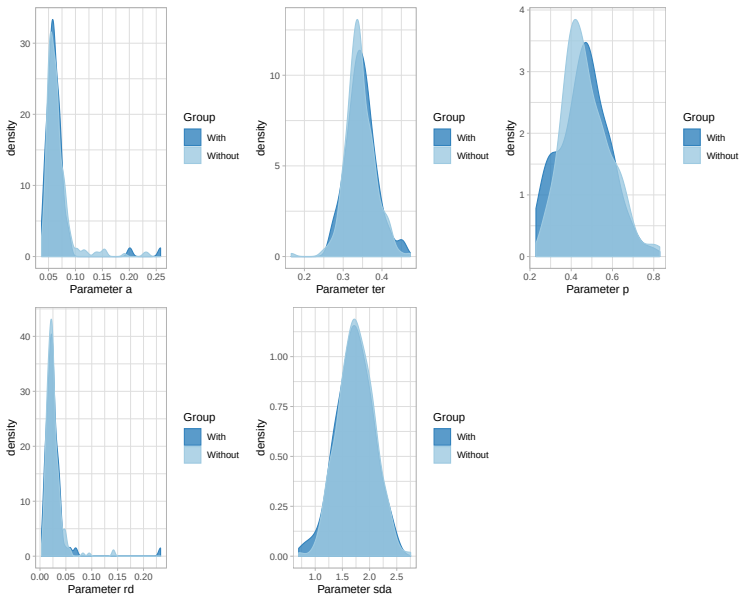

Figure G12. Density distributions of the SSP model parameters in Experiment 2 split by those declaring a depression diagnosis ("with depression") to those who declare no diagnosis of depression ("without depression").

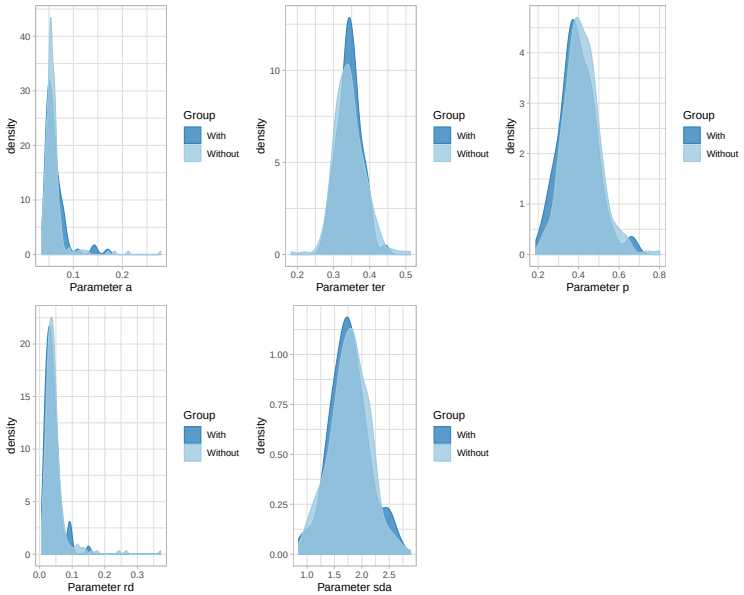

Figure G13. Density distributions of the SSP model parameters in Experiment 3 split by those declaring a depression diagnosis ("with depression") to those who declare no diagnosis of depression ("without depression").

References

Dillon, D. G., Wiecki, R., Pechtel, P., Webb, C., Goer, F., Murray, L., ... Pizzagalli, D. (2015). A computational analysis of flanker interference in depression. *Psychological Medicine*, *45*, 2333–2344. doi: http://dx.doi.org/10.1017/S0033291715000276

Grange, J. A. (2016). flankr: An R package implementing computational models of attentional selectivity. *Behavior Research Methods*, *48*, 528–541. doi: https://doi.org/10.3758/s13428-015-0615-y

Hübner, R., Steinhauser, M., & Lehle, C. (2010). A dual-stage two-phase model of selective attention. *Psychological Review*, *117*, 759–784. doi: https://dx.doi.org/10.1037/a0019471

White, C. N., Ratcliff, R., & Starns, J. J. (2011). Diffusion models of the flanker task: Discrete versus gradual attentional selection. *Cognitive Psychology*, *63*, 210–238. doi: https://doi.org/10.1016/j.cogpsych.2011.08.001